Nuclear spin-isospin excitations within the relativistic energy-density functional framework

Tomohiro Oishi

(YITP, Kyoto University, Japan)

Collaborators:
Nils Paar (Univ. of Zagreb, Croatia)
Ante Ravlic (Univ. of Zagreb, Croatia)
Goran Kruzic (Univ. of Zagreb & Ericsson-Nikola Tesla, Croatia)

Spin magnetic-dipole (M1) = spin-isospin mode A

The spin-M1 operator in its isovector (IV) mode contains the spin-isospin excitation operator.
Selection rule (even-even): 0+ ➔ 1+

$$\hat{\mathcal{O}}^{\mathrm{M1}}_{\nu} = \sum_{k\in A} \hat{\tau}_0(k)\hat{s}_\nu(k),$$

$$\hat{\mathcal{O}}^{\mathrm{GT}(\pm)}_{\nu} = \sum_{k\in A} \hat{\tau}_\pm(k)\hat{s}_\nu(k),$$

In M1 transitions, main contributions stem from the spin-orbit (SO) splitting as well as the relevant residual interactions.

$$\langle \mathcal{Y}_{l'j'} \,||\, \hat{s} \,||\, \mathcal{Y}_{lj} \rangle = \delta_{l'l}(-)^{l+j'+3/2}\sqrt{(2j'+1)(2j+1)} \begin{Bmatrix} 1/2 & j' & l \\ j & 1/2 & J=1 \end{Bmatrix} \cdot \sqrt{\frac{3}{2}}.$$

Only the $j_{>,<}$ ➔ $j_{<,>}$ transition is allowed.

The M1 mode also plays a role in the determination of neutron-capture rates, of significance for the r-process nucleosynthesis.

Gamow-Teller (GT) = spin-isospin mode B

Main component of charge-exchange reactions and beta-radioactivity. Its operator is similar to the M1, and the selection rule is the same but including the charge exchanging (CE).

$$\hat{\mathcal{O}}_{\nu}^{\mathrm{M1}} = \sum_{k\in A} \hat{\tau}_0(k)\hat{s}_{\nu}(k),$$

$$\hat{\mathcal{O}}_{\nu}^{\mathrm{GT}(\pm)} = \sum_{k\in A} \hat{\tau}_{\pm}(k)\hat{s}_{\nu}(k),$$

B(GT) ← Two experimental probes have been utilized:

- Weak-interaction probe = beta radioactivity.
- Strong-interaction probe = CE reactions, e.g. by proton or He-3 scattering.

GT transitions → (i) nucleosynthesis, especially by determining the beta-decay lifetimes, which provide a key ingredient for understanding the r-process timescale; (ii) neutrino-induced reactions and electron capture in nuclei during the late stages of stellar evolution; (iii) double-beta decays(?).

M1 and GT transitions

E.g. ^{42}Ca ~= ^{40}Ca+2n

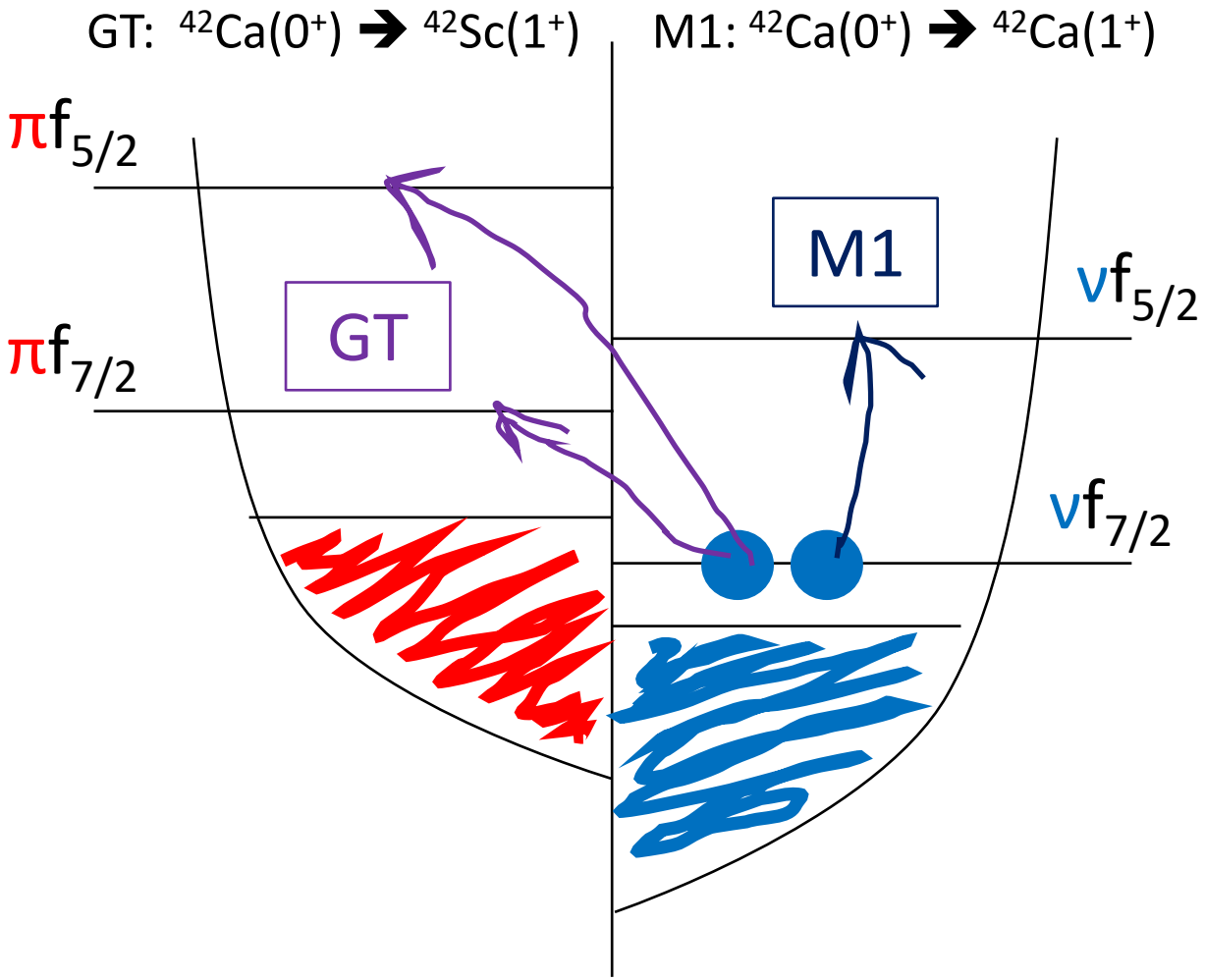

$$\hat{\mathcal{O}}_{\nu}^{\mathrm{M1}} = \sum_{k\in A} \hat{\tau}_0(k)\hat{s}_{\nu}(k),$$

$$\hat{\mathcal{O}}_{\nu}^{\mathrm{GT}(\pm)} = \sum_{k\in A} \hat{\tau}_{\pm}(k)\hat{s}_{\nu}(k),$$

E(M1) ~= E(νf$_{5/2}$) - E(νf$_{7/2}$), whereas ΔE(GT) ~= E(πf$_{5/2}$) - E(πf$_{7/2}$), with common selection rule: 0$^+$ ➔ 1$^+$.

M1 & GT can be interpreted as isobaric-analogue transitions. Does the theory reproduces them simultaneously? (LS splitting, res. interactions, pairing, etc.)

Model & Setting

My tools:

- Relativistic energy-density functional (REDF) theory;
- Mean-field calculation of the relativistic Hartree-Bogoliubov (RHB) type with DD-PC1;
- Relativistic quasi-particle random-phase approximation (QRPA) for M1/GT excitations;
- IV-PV residual interaction & pairing interaction.

Energy-density functional (EDF) theory

The nuclear EDF theory has been utilized as one tool to calculate the nuclear properties widely in the nuclear chart.

- Non-rela' EDF: Skyrme, Gogny, etc.
- Rela' EDF: meson-exchange or point-coupling.

Implementation:

- Ground states: the self-consistent EDF-meanfield (HFB) calculation.
- Dynamical properties, e.g. collective excitations: the quasi-particle random-phase approximation (QRPA), time-dependent EDF, etc.

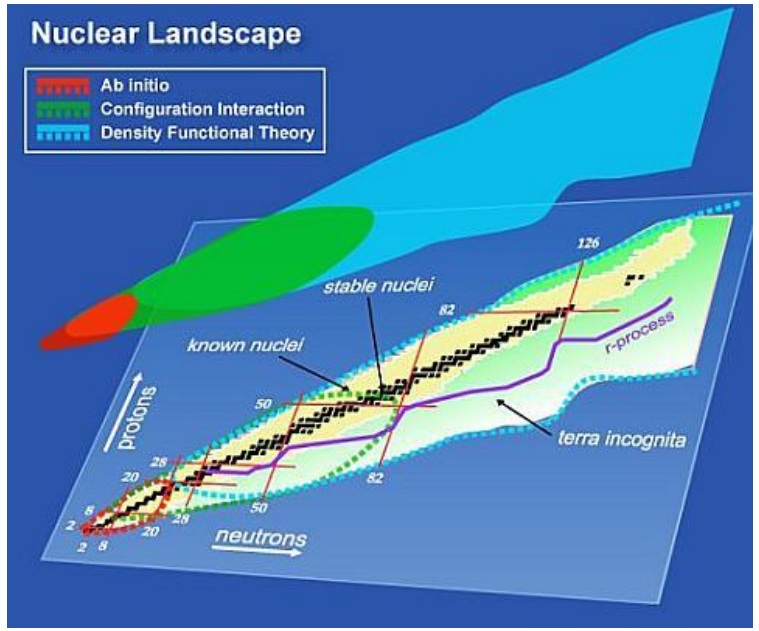

H. Nam et al, J. of Phys. Conf. Series 401, 012033 (2012).

QRPA equation (matrix formulation)

$$[\hat{H}', \hat{O}^\dagger_\lambda] = \omega_\lambda \hat{O}^\dagger_\lambda \quad \Longleftrightarrow \quad \begin{pmatrix} A & B \\ B^* & A^* \end{pmatrix} \begin{pmatrix} X^\lambda \\ Y^\lambda \end{pmatrix} = \omega_\lambda \begin{pmatrix} X^\lambda \\ -Y^\lambda \end{pmatrix}$$

phonon operator:

$$\hat{O}^\dagger_\lambda = \sum_{\mu\nu} X^\lambda_{\mu\nu} \hat{a}^\dagger_\mu \hat{a}^\dagger_\nu - Y^\lambda_{\mu\nu} \hat{a}_\nu \hat{a}_\mu$$

Normalization:

$$\sum_{\mu<\nu} X^\lambda_{\mu\nu} X^{\lambda'*}_{\mu\nu} - Y^\lambda_{\mu\nu} Y^{\lambda'*}_{\mu\nu} = \delta_{\lambda\lambda'}$$

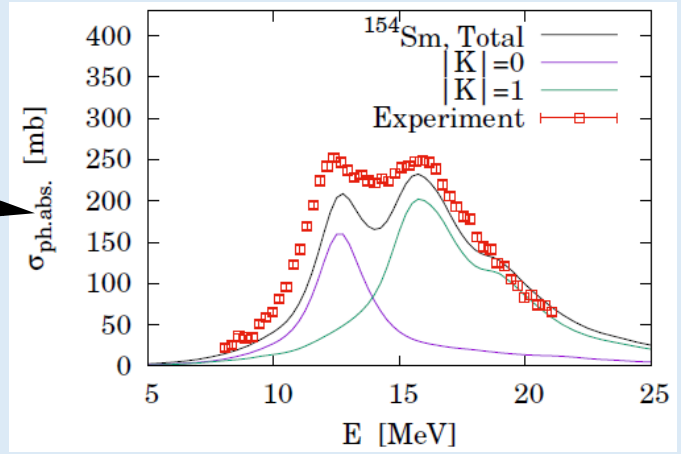

What “relativistic” DFT provides?

Relativistic EDF (Covariant DF) Theory
= effective field theory of nucleons and mesons.

$$
\begin{aligned}
\mathcal{L}_{\mathrm{REDF}} &= \bar{\psi}(x)\left[i\,\partial\!\!\!/ - m\right]\psi(x) \\
&\quad + \mathcal{L}_{\mathrm{meson}} + \mathcal{L}_{\mathrm{int}}, \ \text{where} \\
\psi(x) &\cdots \text{nucleon}, \\
\mathcal{L}_{\mathrm{meson}} &\cdots \text{free mesons}, \\
\mathcal{L}_{\mathrm{int}} &\cdots \text{interactions}.
\end{aligned}
$$

Motivation & Caution to choose the REDF framework:

- ✓ In the original work by J.D. Walecka [1], his original motivation was to obtain the stress tensor for the Einstein equation of neutron stars. This purpose needs the relativistic formalism. As a successful result by Walecka [1], the repulsive core of the nuclear force in the high-density region can be naturally concluded.
- ✓ The Dirac-Lorentz formalism leads to a consistent treatment of spin degrees of freedom as well as an unified description of time-even and time-odd fields [2]. Also, the relativistic effect and causality can be included [1-4].
- ✓ Connection between the force and meson is clear: e.g. tensor force is from one-pion exchange (pseudo-scalar & pseudo-vector coupling) [4].
- ✓ Spin-orbit (LS) level splitting, which is one fundamental feature of atomic nuclei, is naturally concluded [2-4]. This character is linked to e.g. the M1 and Gamow-Teller excitations.

References: [1] J. D. Walecka, Ann. of Phys. 83, 491 (1974); [2] D. Vretenar et al., Phys. Report 409, 101-259 (2005); [3] P.-G. Reinhard, Rep. on Progress in Phys. 52, 439 (1989); [4] 土岐博＆保坂淳、「相対論的多体系としての原子核」、大阪大学出版会(2011).

Spin-orbit (LS) splitting from Dirac eq.

$$\left[-i\hbar c\beta\vec{\gamma}\cdot\vec{\nabla}+\beta Mc^2+\beta S(r)+W(r)\right]\psi_N(t,\boldsymbol{r})=E_N\psi_N(t,\boldsymbol{r}).$$

Scalar meson(s)

Vector meson(s)

$$\psi_N(\boldsymbol{r})=\psi_{nljm}(\boldsymbol{r})=\begin{pmatrix} iF_N(\boldsymbol{r}) \\ \\ G_N(\boldsymbol{r}) \end{pmatrix}=\begin{pmatrix} if_{nlj}(r)\mathcal{Y}_{ljm}(\bar{\boldsymbol{r}}) \\ \\ g_{nlj}(r)\frac{\vec{\sigma}\cdot\boldsymbol{r}}{r}\mathcal{Y}_{ljm}(\bar{\boldsymbol{r}}) \end{pmatrix}$$

$$\left[-\frac{(\hbar c)^2}{\epsilon_N(r)}\nabla^2-(\hbar c)^2\frac{(-)\epsilon_N'(r)}{\epsilon_N^2(r)}\frac{d}{dr}+\frac{(\hbar c)^2}{r}\frac{(-)\epsilon_N'(r)}{\epsilon_N^2(r)}\frac{2\vec{S}\cdot\vec{L}}{\hbar^2}\right.$$

$$\left.+S(r)+W(r)\right]F_N(\boldsymbol{r}) \;=\; (E_N-Mc^2)F_N(\boldsymbol{r}),$$

where the 1st term in the LHS corresponds to the kinetic energy, the 2nd term is so-called Darwin term, and the 3rd term indicates the spin-orbit coupling. These Darwin and spin-orbit terms can be naturally concluded from the Dirac equation, whereas those were just introduced as "phenomenology" in the Schroedinger equation.

It is convenient to find that,

- the total potential is given as $S(r)+W(r)$, whereas,
- the spin-orbit and Darwin terms depend on the $\epsilon_N'(r)=S'(r)-W'(r)$.

M1 and GT transitions

E.g. ^{42}Ca ~= ^{40}Ca+2n

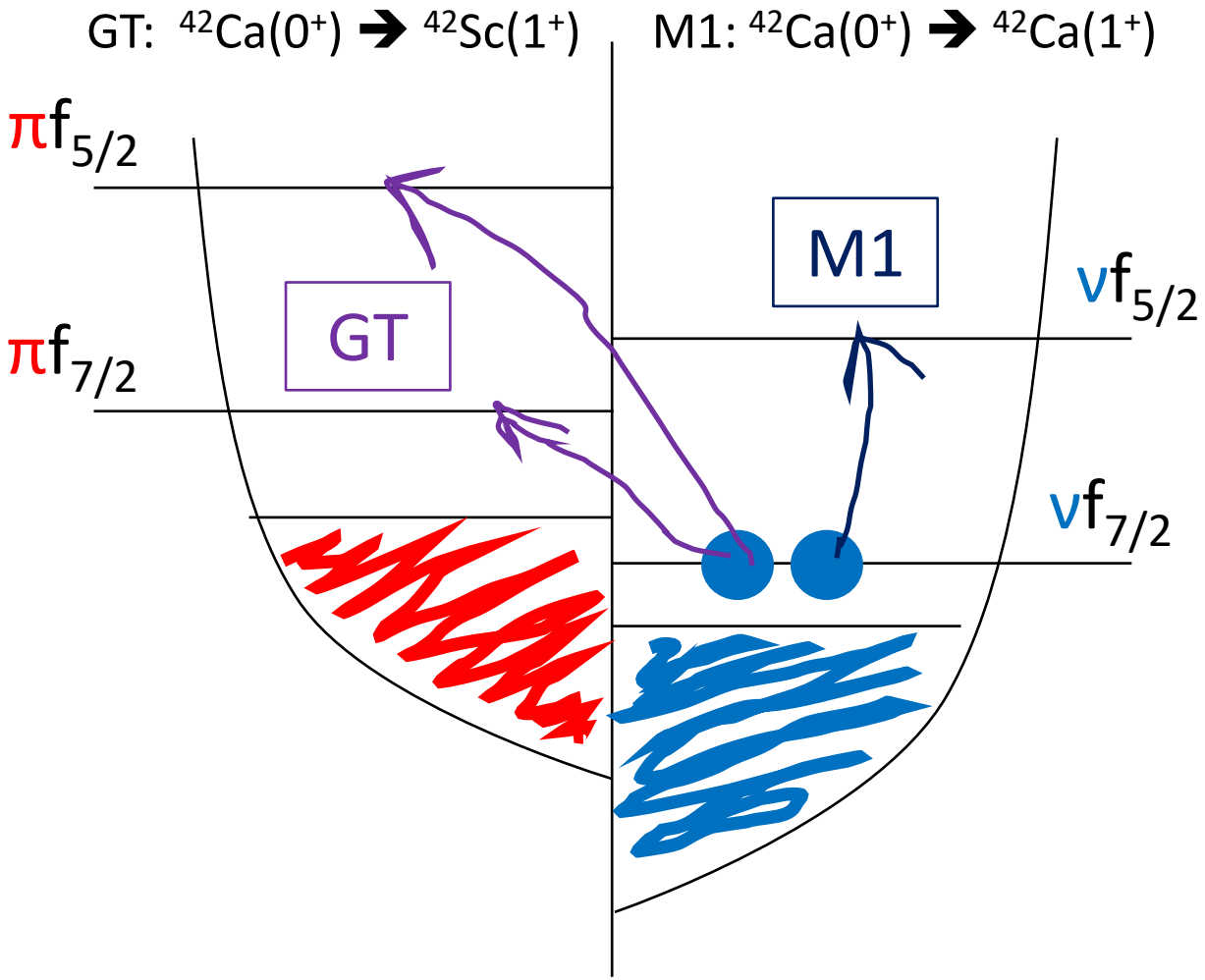

$$\hat{\mathcal{O}}_{\nu}^{\mathrm{M1}} = \sum_{k\in A} \hat{\tau}_0(k)\hat{s}_{\nu}(k),$$

$$\hat{\mathcal{O}}_{\nu}^{\mathrm{GT}(\pm)} = \sum_{k\in A} \hat{\tau}_{\pm}(k)\hat{s}_{\nu}(k),$$

E(M1) ~= E(νf$_{5/2}$) - E(νf$_{7/2}$), whereas ΔE(GT) ~= E(πf$_{5/2}$) - E(πf$_{7/2}$), with common selection rule: 0$^+$ ➔ 1$^+$.

M1 & GT can be interpreted as isobaric-analogue transitions. Does the theory reproduces them simultaneously? (LS splitting, res. interactions, pairing, etc.)

Point-Coupling REDF Lagrangian

In the relativistic nuclear theory (RNT), nucleon is described by a Dirac spinor $\psi(x)$, where $x = \{\boldsymbol{r}, \boldsymbol{s}, \vec{\tau}\}$. The phenomenological Lagrangian density reads

$$\mathcal{L} = \bar{\psi}(x)[i\gamma_\mu\partial^\mu - M]\psi(x) + \mathcal{L}_{\rm M} + \mathcal{L}_{\rm I}. \qquad (1)$$

TABLE 2: Interaction terms included in $\mathcal{L}_{\rm I}$. Label (i) indicates isoscalar (IS) or isovector (IV). Label (ii) indicates scalar (S), vector (V), pseudo-scalar (PS) or pseudo-vector (PV).

(i)	(ii)	(T, J^π)	Meson	Meson-exchange	Point-coupling
IS	S	$(0, 0^+)$	σ	$-g_\sigma\bar{\psi}\sigma\psi$	$-\alpha_{\rm IS-S}(\rho)[\bar{\psi}\psi][\bar{\psi}\psi]/2$
					$-\delta_{\rm IS-S}(\rho)\partial_\mu[\bar{\psi}\psi]\partial^\mu[\bar{\psi}\psi]/2$
	V	$(0, 1^-)$	ω^μ	$-g_\omega[\bar{\psi}\gamma_\mu\omega^\mu\psi]$	$-\alpha_{\rm IS-V}(\rho)[\bar{\psi}\gamma_\mu\psi][\bar{\psi}\gamma^\mu\psi]/2$
	PS	$(0, 0^-)$	$\times$	$\times$	$\times$
	PV	$(0, 1^+)$	$\times$	$\times$	$\times$
IV	S	$(1, 0^+)$	$\times$	$\times$	$\times$
	V	$(1, 1^-)$	$\vec{\rho}^\mu$	$-g_\rho[\bar{\psi}\gamma_\mu(\vec{\tau}\vec{\rho}^\mu)\psi]$	$-\alpha_{\rm IV-V}(\rho)[\bar{\psi}\gamma_\mu\vec{\tau}\psi][\bar{\psi}\gamma^\mu\vec{\tau}\psi]/2$
	PS	$(1, 0^-)$	$\vec{\pi}$	$-ig_\pi[\bar{\psi}\gamma_5(\vec{\tau}\vec{\pi})\psi]$	$-\alpha_{\rm IV-PS}(\rho)[\bar{\psi}\gamma_5\vec{\tau}\psi][\bar{\psi}\gamma_5\vec{\tau}\psi]/2$
	PV	$(1, 1^+)$	$\partial_\mu\vec{\pi}$	$-\frac{f_\pi}{m_\pi}[\bar{\psi}\gamma_5\gamma_\mu\partial^\mu(\vec{\tau}\vec{\pi})\psi]$	$-\alpha_{\rm IV-PV}(\rho)[\bar{\psi}\gamma_5\gamma_\mu\vec{\tau}\psi][\bar{\psi}\gamma_5\gamma^\mu\vec{\tau}\psi]/2$
Coulomb					$-e\bar{\psi}\gamma_\mu A^\mu\left(\frac{1-\hat{\tau}_3}{2}\right)\psi$

In this work, we employ the point-coupling model.

Setting = DD-PC1 parameters.

Refs:
[1] T. Niksic, D. Vretenar, and P. Ring, Progress in Particle and Nuclear Physics 66(3), 519-548 (2011). [2] T. Niksic et. al., Comp. Phys. Communications, 107184 (2020).

Method = Relativistic Hartree-Bogoliubov & QRPA

Point-coupling REDF Lagrangian: $\mathcal{L} = \bar{\psi}(x)[i\gamma_\mu\partial^\mu - M]\psi(x) + \mathcal{L}_{\rm M} + \mathcal{L}_{\rm I}.$

$$\mathcal{L}_I = -\frac{\alpha_{\rm IS-S}(\rho)}{2}[\bar{\psi}\psi][\bar{\psi}\psi] - \frac{\alpha_{\rm IS-V}(\rho)}{2}[\bar{\psi}\gamma_\mu\psi][\bar{\psi}\gamma^\mu\psi] - \frac{\alpha_{\rm IV-V}(\rho)}{2}[\bar{\psi}\gamma_\mu\vec{\tau}\psi][\bar{\psi}\gamma^\mu\vec{\tau}\psi]$$ DD-PC1

$$- \frac{\alpha_{\rm IV-PV}(\rho)}{2}[\bar{\psi}\gamma_5\gamma_\mu\vec{\tau}\psi][\bar{\psi}\gamma_5\gamma^\mu\vec{\tau}\psi] - e\bar{\psi}\gamma_\mu A^\mu\left(\frac{1-\hat{\tau}_3}{2}\right)\psi$$ IV-PV for RQRPA

- ✓ (i) For the GS of even-even nuclei, the relativistic Hartree-Bogoliubov (RHB) calculation is performed by using the DD-PC1 setting of Lagrangian parameters [1, 2]. (ii) Gogny-D1S pairing is also used for the particle-particle channel [3]. (iii) For the M1-excited states, the relativistic QRPA is employed [3].

QRPA: $\begin{pmatrix} A & B \\ -B^* & -A^* \end{pmatrix}\begin{pmatrix} X^\nu \\ Y^\nu \end{pmatrix} = \omega_\nu \begin{pmatrix} X^\nu \\ Y^\nu \end{pmatrix}$. $\frac{dB_{\rm M1}}{dE_\gamma} = \sum_i \delta(E_\gamma - \hbar\omega_i)\sum_\nu \left|\left\langle \omega_i \left| \hat{\mathcal{Q}}_\nu({\rm M1}) \right| \Phi \right\rangle\right|^2$

- ✓ In the M1-QRPA, we additionally consider the IV-PV coupling as the residual interaction [3]. Note that this IV-PV originates in the one-pion exchange.

References: [1] T. Niksic, D. Vretenar, and P. Ring, Progress in Particle and Nuclear Physics 66(3), 519-548 (2011). [2] T. Niksic et. al., Comp. Phys. Communications, 107184 (2020). [3] G. Kruzic et. al., Phys. Rev. C 102, 044315 (2020).

Calculations & Results

$$\hat{\mathcal{H}}\,|\omega\rangle = \hbar\omega\,|\omega\rangle\,, \qquad |\omega\rangle = \hat{\mathcal{Z}}^{\dagger}(\omega)\,|\Phi\rangle\,, \quad \hat{\mathcal{Z}}^{\dagger}(\omega) = \frac{1}{2}\sum_{\rho\neq\sigma}\left\{X_{\rho\sigma}(\omega)\hat{\mathcal{Q}}^{\dagger}_{\sigma\rho} - Y^{*}_{\rho\sigma}(\omega)\hat{\mathcal{Q}}_{\sigma\rho}\right\},$$

$$\begin{pmatrix} A & B \\ B^{*} & A^{*} \end{pmatrix}\begin{pmatrix} X(\omega) \\ Y^{*}(\omega) \end{pmatrix} = \hbar\omega\begin{pmatrix} I & 0 \\ 0 & -I \end{pmatrix}\begin{pmatrix} X(\omega) \\ Y^{*}(\omega) \end{pmatrix}$$

$$R_X(E) = \sum_f \delta(E - E_f) B_X(E_f)$$

$$= \sum_f \delta(E - E_f) \sum_{\nu=\pm1,0} \left|\left\langle f \mid \hat{\mathcal{O}}^{X}_{\nu} \mid \Phi \right\rangle\right|^2$$

Non-pertub. calculations for M1/GT transitions

$$R(E) = \sum_f \delta(E - E_f) \sum_{\nu=\pm1,0} \left| \left\langle f \mid \hat{\mathcal{O}}^X_\nu \mid \Phi \right\rangle \right|^2$$

Non-perturbed calculations of Rela' QRPA, where DD-PC1 Lagrangian is used.

No residual interactions:

- IV-PV ➔ Neglected.
- Pairing ➔ Neglected.

$$\hat{\mathcal{O}}^{\mathrm{IVM1}}_\nu = \frac{\mu_N}{4\pi} \sum_{k\in A} \hat{\tau}_0(k)\hat{s}_\nu(k),$$

$$\hat{\mathcal{O}}^{\mathrm{GT}(\pm)}_\nu = \sum_{k\in A} \hat{\tau}_\mp(k)\hat{s}_\nu(k),$$

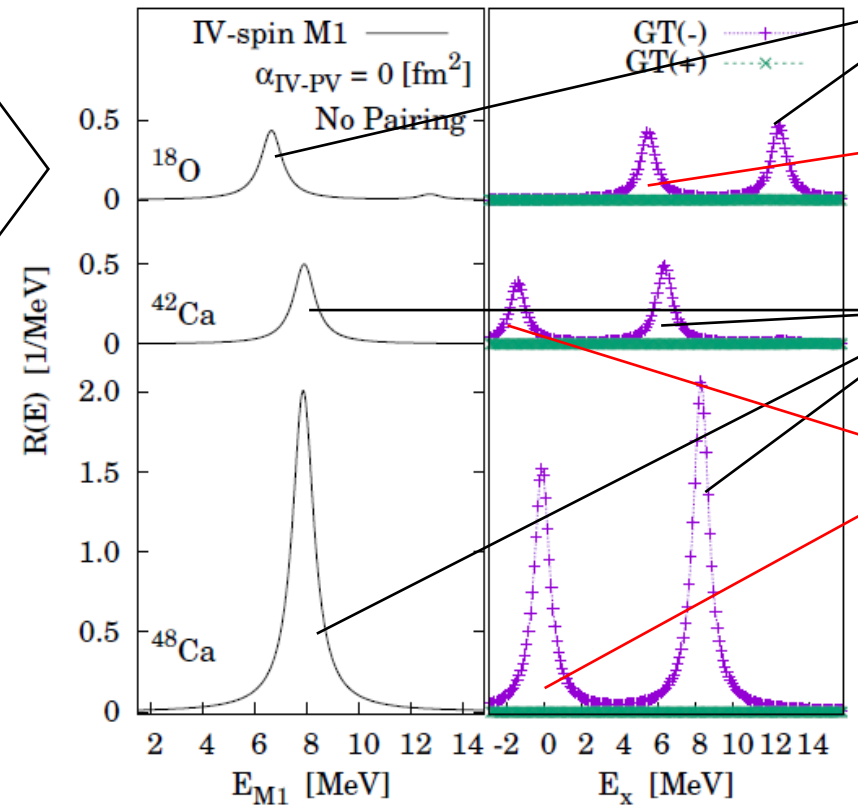

FIG. 1. Non-perturbed IV-spin M1 and GT(±) strength distributions obtained with RQRPA method, where residual interactions are neglected. The GT(±) energies E_x are presented with respect to the daughter nuclei.

$\nu(1d_{5/2}) \longrightarrow \nu(1d_{3/2})$ in IV M1, and
$\nu(1d_{5/2}) \longrightarrow \pi(1d_{3/2})$ in GT(−),

$\nu(1d_{5/2}) \longrightarrow \pi(1d_{5/2})$ in GT(−),

$\nu(1f_{7/2}) \longrightarrow \nu(1f_{5/2})$ in IV M1, and
$\nu(1f_{7/2}) \longrightarrow \pi(1f_{5/2})$ in GT(−).

$\nu(1f_{7/2}) \longrightarrow \pi(1f_{7/2})$ in GT(−).

- ✓ Equivalence between M1 and higher GT(-) is confirmed.
- ✓ GT(-) has another low-lying resonance.
- ✓ Ikeda-Fujita-Fujii SR for GT ➔ Checked.
- ✓ Kurath's SR for M1 ➔ Checked.

➔ Let's see what happens when we add residual interactions.

Non-pertub. calculations for M1/GT transitions

$R(E) = \sum_f \delta(E$

Non-pertu
calculatio
QRPA, wh
Lagrangia

No residu
- IV-PV
- Pairing

$\hat{\mathcal{O}}_\nu^{\mathrm{IVM1}} =$

$\hat{\mathcal{O}}_\nu^{\mathrm{GT}(\pm)} =$

TABLE I. Interactions used in our RHB and RQRPA calculations. The label ph (pp) indicates the quasi-particle quasi-hole (quasi-particle quasi-particle) channel.

		M1	GT
RHB (0^+)	ph	DD-PC1	
	pp	T1 pairing	
RQRPA (1^+)	ph	DD-PC1 plus IV-PV	
	pp	T1 pairing	PN pairing

$$\mathcal{L} = \mathcal{L}_{\mathrm{DD-PC1}} + \mathcal{L}_{\mathrm{IV-PV}}, \quad \mathcal{L}_{\mathrm{IV-PV}} = -\hbar c \frac{\alpha_{\mathrm{IV-PV}}}{2} \left[\bar{\psi}\gamma_5\gamma_\mu\vec{\tau}\psi\right]\left[\bar{\psi}\gamma_5\gamma^\mu\vec{\tau}\psi\right].$$

If open shell, $V_{\mathrm{pp,T0}}(d) = \sum_{i=1,2} U_i(S_{12}) e^{-d^2/\mu_i^2}$

$V_{\mathrm{pp,T1}}(d) = \sum_{i=1,2} V_i(S_{12}) e^{-d^2/\mu_i^2}$, where $d = |\boldsymbol{r}_2 - \boldsymbol{r}_1|$

FIG. 1. Non-perturbed IV-spin M1 and GT(±) strength distributions obtained with RQRPA method, where residual interactions are neglected. The GT(±) energies E_x are presented with respect to the daughter nuclei.

➔ Let's see what happens when we add residual interactions.

REDF calculations for M1 and GT transitions

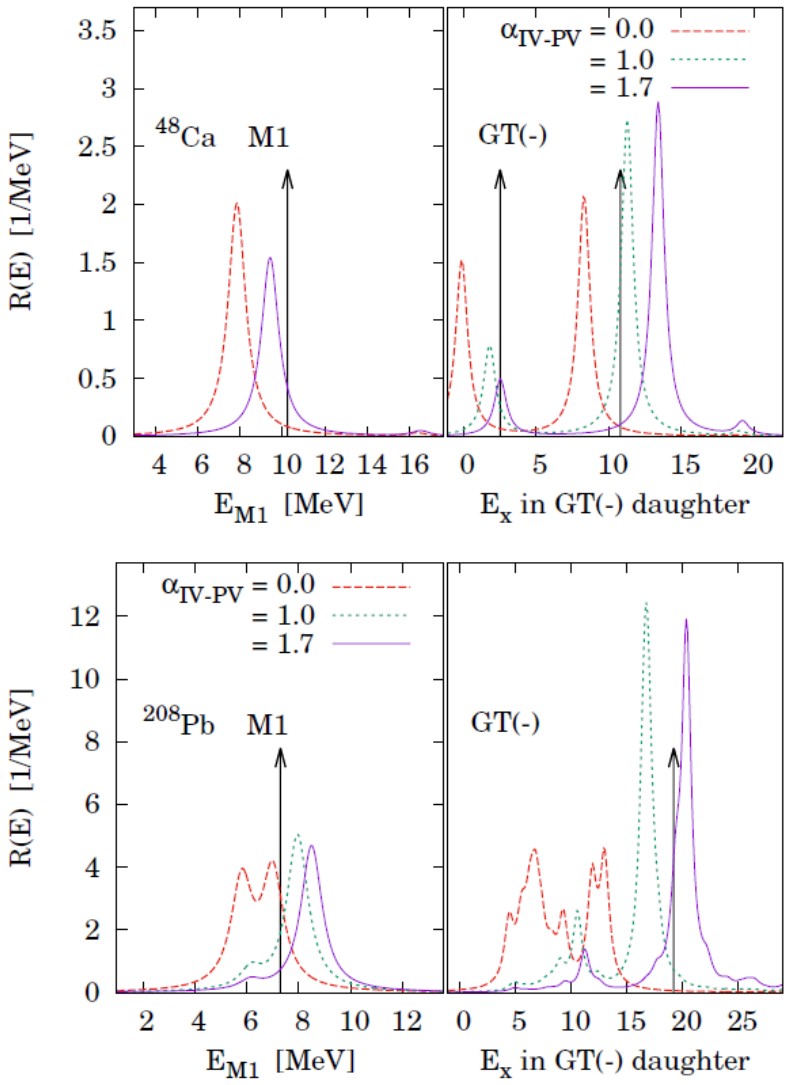

$$R(E) = \sum_f \delta(E - E_f) \sum_{\nu=\pm1,0} \left| \left\langle f \mid \hat{\mathcal{O}}^X_\nu \mid \Phi \right\rangle \right|^2$$

← Rela' QRPA with DD-PC1 plus IV-PV.

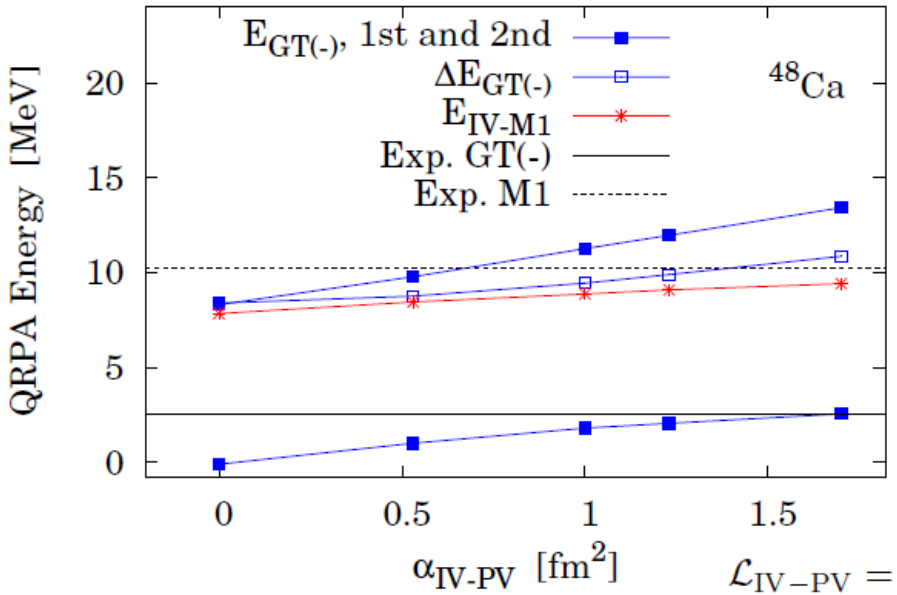

$$\hat{\mathcal{O}}^{IVM1}_\nu = \frac{g_s \mu_N}{2}\sqrt{\frac{3}{4\pi}} \sum_{k\in A} \hat{\tau}_0(k)\hat{s}_\nu(k),$$

$$\hat{\mathcal{O}}^{GT(\pm)}_\nu = \sum_{k\in A} \hat{\tau}_\mp(k)\hat{s}_\nu(k),$$

$$\mathcal{L}_{IV-PV} = -\hbar c \frac{\alpha_{IV-PV}}{2} \left[\bar{\psi}\gamma_5\gamma_\mu\vec{\tau}\psi\right]\left[\bar{\psi}\gamma_5\gamma^\mu\vec{\tau}\psi\right]$$

➔ As the residual IV-PV interaction becomes stronger, the M1 and GT get more divergent from each other. Namely, the IV-PV interaction disrupts the isobaric-analogue similarity between M1 and GT.

➔ In parallel, the simultaneous reproduction of M1 & GT for light-heavy nuclei is still demanding, and we are working on this.

Mirror symmetry of M1 and GT transitions

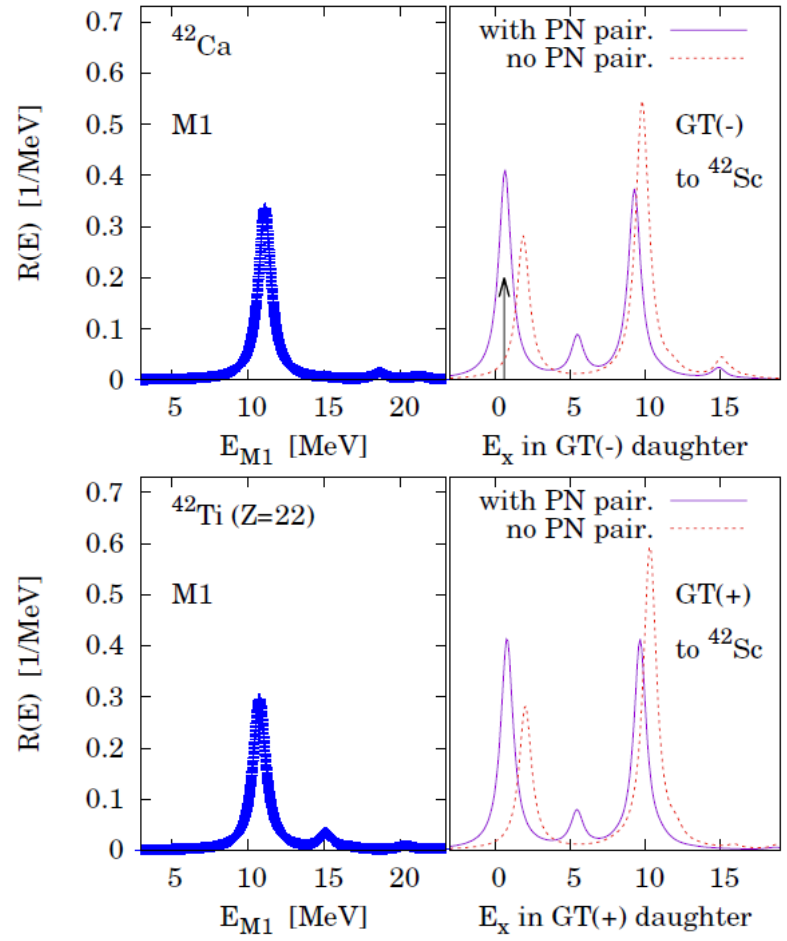

FIG. 5. The M1 and GT strength distributions of ^{42}Ca and ^{42}Ti. For GT(±) modes, their excitation energies are presented with respect to the common daughter nucleus ^{42}Sc. The arrow indicates the experimental low-lying GT(−) energy 0.611 MeV in ^{42}Sc [37].

"Colourful Nuclide Chart"

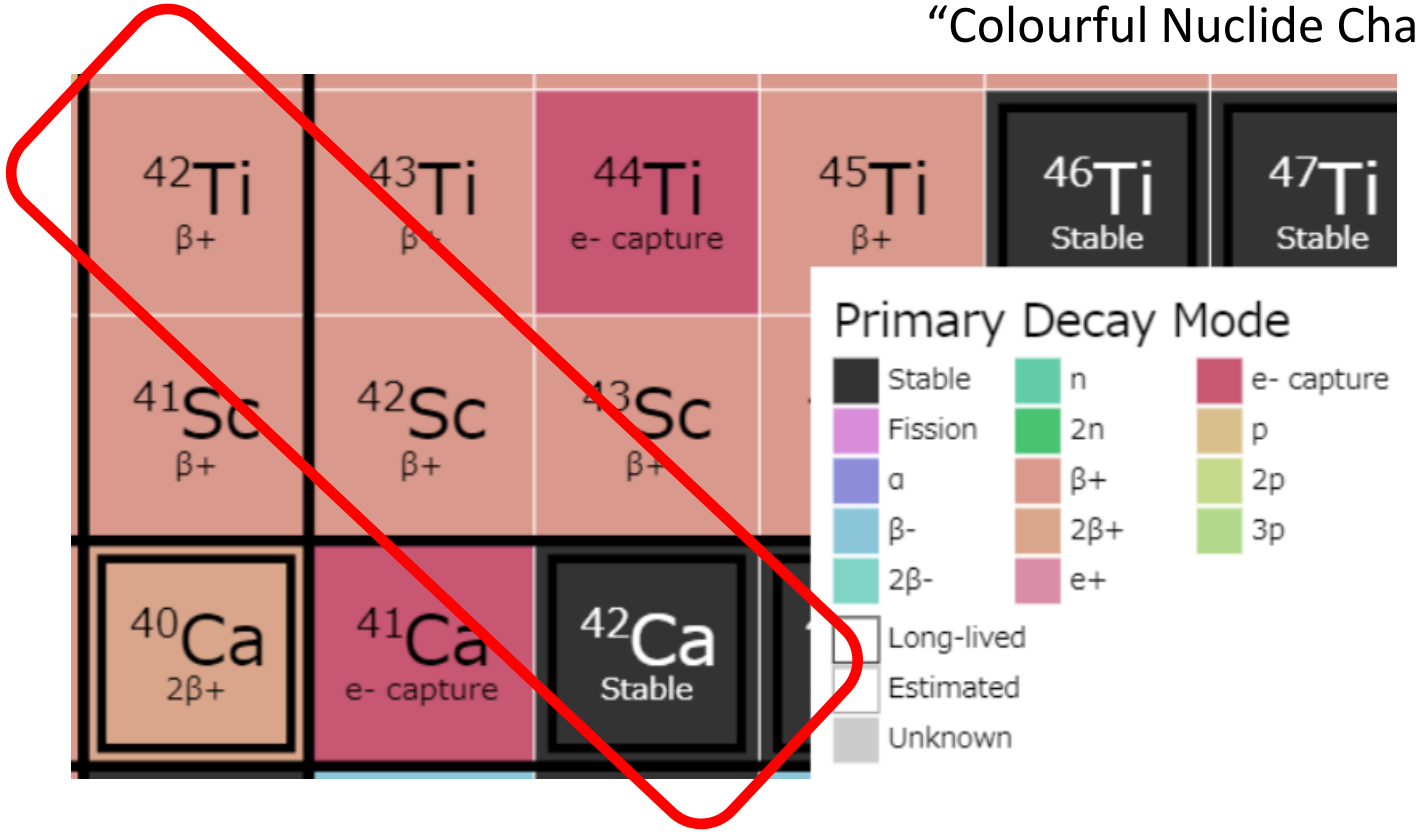

✓ Both M1 and GT(+)(-) transitions show an agreement between mirror-symmetric nuclei. Here pairing is taken into account.

Mirror symmetry of M1 and GT transitions

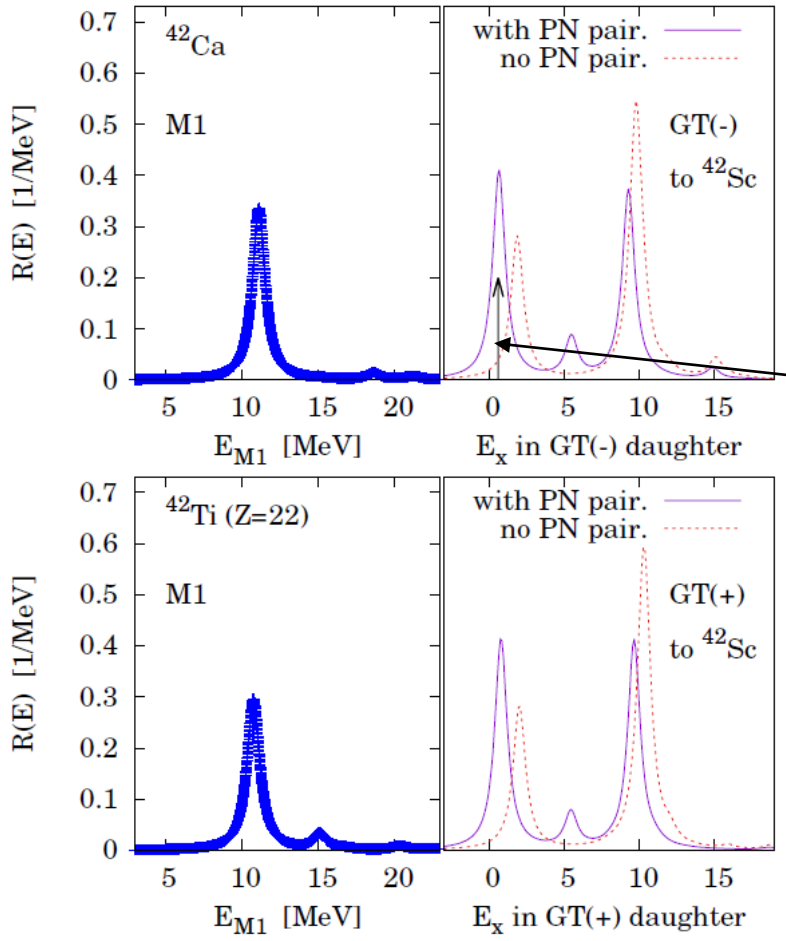

FIG. 5. The M1 and GT strength distributions of ^{42}Ca and ^{42}Ti. For GT(±) modes, their excitation energies are presented with respect to the common daughter nucleus ^{42}Sc. The arrow indicates the experimental low-lying GT(−) energy 0.611 MeV in ^{42}Sc [37].

Experimental data by Y. Fujita et al, Eur. Phys. J. A 56, 138 (2020): E_{GT} = 0.611 MeV.

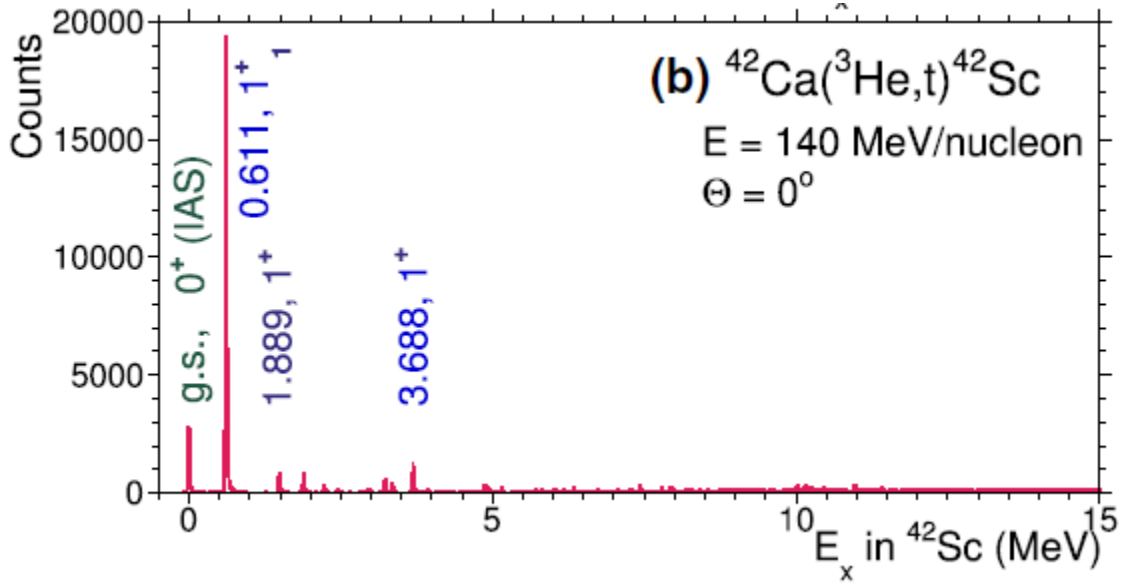

- ✓ Both M1 and GT(+)(-) transitions show an agreement between mirror-symmetric nuclei. Here pairing is taken into account.
- ✓ PN-pairing plays an essential role to explain the low-lying GT peaks.
- ✓ Giant GT somehow vanishes in experiments. Continuum effect?

Mirror symmetry of M1 and GT transitions

Ikeda-Fujii-Fujita Sumrule:

$$\lim_{E_x \to \infty} \left[S_{\mathrm{GT}(-)}(E_x) - S_{\mathrm{GT}(+)}(E_x) \right] = \frac{3(N-Z)}{4},$$

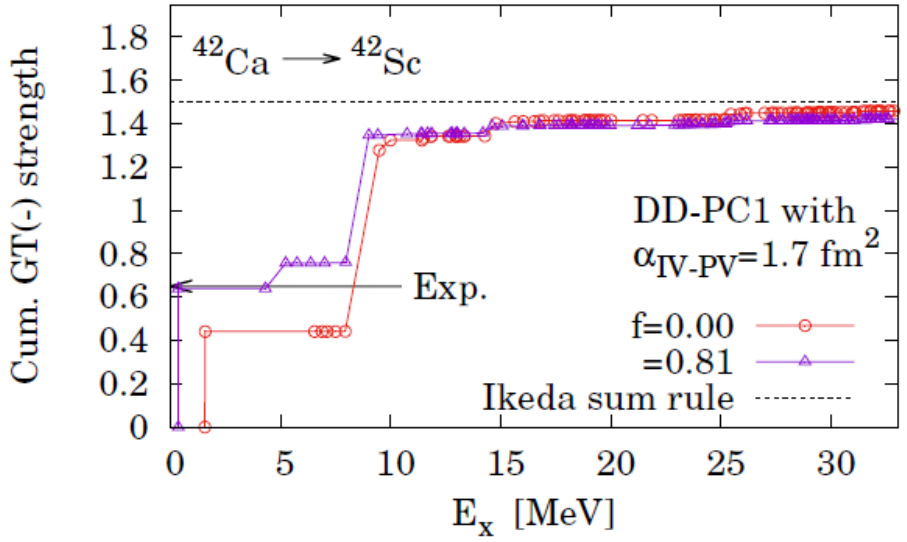

Figure 6. Cumulative GT(−) strength for ^{42}Ca obtained with the DD-PC1 plus IV-PV interaction with $\alpha_{\mathrm{IV-PV}} = 1.7$ fm^2. Ikeda-Fujii-Fujita sum rule as in Eq. (14) is plotted by the dotted line. The arrow indicates the experimental value of $\sum B_{\mathrm{GT}(-)} = 2.6/4$ [55].

- ✓ Both M1 and GT(+)(-) transitions show an agreement between mirror-symmetric nuclei. Here pairing is taken into account.
- ✓ PN-pairing plays an essential role to explain the low-lying GT peaks.
- ✓ Giant GT somehow vanishes in experiments. Continuum effect?

Summary

The relativistic HB+QRPA computation is applied to the M1 and GT excitations.

- ✓ The IV-PV coupling remarkably shifts the M1 and GT-excitation properties.
- ✓ For simultaneous reproduction of M1 and GT of various nuclei, we need to improve the REDF Lagrangian, e.g., with the more density-dependent couplings to reproduce the M1/GT energies of doubly-magic nuclei.
- ✓ The pairing interactions provide a sizable effect on these spin-isospin transitions. The spin-singlet (S_{12}=0) pairing picture for NN and PP provides a better option to reproduce the experimental M1 data of open-shell nuclei. The PN pairing is, on the other side, important to explain the low-lying GT excitations.

Future works:

- ✓ Improvement of the REDF parameters. The experimental data on the M1 and GT may be a suitable reference.
- ✓ Neutron-rich and proton-rich, and/or deformed nuclei.
- ✓ Collaborations with (i) quantum computing and (ii) AI technologies for REDF calculations.

Acknowledgement

This work was supported by the QuantiXLie Centre of Excellence, a project co-financed by the Croatian Government and European Union through the European Regional Development Fund - the Competitiveness and Cohesion Operational Program (Grant KK.01.1.1.01.0004).
For more information please visit: http://bela.phy.hr/quantixlie/hr/
https://strukturnifondovi.hr/
The sole responsibility for the content of this presentation lies with the Faculty of Science, University of Zagreb. It does not necessarily reflect the opinion of the European Union.

Europska unija
Zajedno do fondova EU

EUROPSKI STRUKTURNI I INVESTICIJSKI FONDOVI

Operativni program KONKURENTNOST I KOHEZIJA

Co-financed by the European Union through the Eurpoean Regional Development Fund

MINISTARSTVO ZNANOSTI I OBRAZOVANJA REPUBLIKE HRVATSKE

MINISTARSTVO REGIONALNOG RAZVOJA I FONDOVA EUROPSKE UNIJE

Sveučilište u Zagrebu

App 1:
Relativistic QRPA for M1

Publications:

1. G. Kruzic, T.O., D. Vale, and N. Paar, Phys. Rev, C 102, 044315 (2020);
2. T.O., G. Kruzic, and N. Paar, J. Phys. G 47, 115106 (2020);
3. G. Kruzic, T.O., and N. Paar, PRC 103, 054306 (2021).

M1 excitation

$$\hat{\mathcal{Q}}(M1,0) = \mu_{\rm N}\sqrt{\frac{3}{4\pi}}(g_l\hat{l}_0 + g_s\hat{s}_0),$$

$$\hat{\mathcal{Q}}(M1,\pm) = (\mp)\mu_{\rm N}\sqrt{\frac{3}{4\pi}}(g_l\hat{l}_\pm + g_s\hat{s}_\pm),$$

Matrix elements of M1 up to the 1-body-operator level:

$$\langle \mathcal{Y}_{l'j'} \,||\, \hat{s} \,||\, \mathcal{Y}_{lj}\rangle = \delta_{l'l}(-)^{l+j'+3/2}\sqrt{(2j'+1)(2j+1)} \begin{Bmatrix} 1/2 & j' & l \\ j & 1/2 & J=1 \end{Bmatrix} \cdot \sqrt{\frac{3}{2}}.$$

$$\left\langle \mathcal{Y}_{l'j'} \,||\, \hat{l} \,||\, \mathcal{Y}_{lj} \right\rangle = (-)^{l'+j+3/2}\sqrt{(2j'+1)(2j+1)} \begin{Bmatrix} l' & j' & 1/2 \\ j & l & J=1 \end{Bmatrix} \cdot \left\langle Y_{l'} \,||\, \hat{l} \,||\, Y_l \right\rangle,$$

where $\left\langle Y_{l'} \,||\, \hat{l} \,||\, Y_l \right\rangle = \delta_{l'l}\sqrt{(2l+1)(l+1)l}.$

➔ The M1 transition happens mainly for the LS-partner levels (*), e.g. $f_{7/2}$ → $f_{5/2}$.
(*) The REDF theory naturally concludes the LS splitting from the Dirac formalism.

How about the ground-state (GS) properties?

Relativistic EDF (Covariant DF) Lagrangian
= density-dependent point-coupling (DD-PC) effective field theory of nucleons.

$$\mathcal{L} = \mathcal{L}_{\mathrm{DD-PC1}} + \mathcal{L}_{\mathrm{IV-PV}},$$

+

- Self-consistent mean-field assumption for single Slater determinant of (quasi-particle) A nucleons.
- For the pp channel, the driving force of Cooper-pairing correlation is approximated with the non-relativistic finite-range force.
- We neglect the Fock terms, and re-optimize the DD-PC Lagrangian. ➔ Self-consistent Dirac-Hartree-Bogoliubov calculation with HO basis.

✓ One relativistic-synonym method of model calculation being similar to the HFB with Skyrme or Gogny force.
✓ Binding energies, their odd-even staggering, and charge radii of medum-heavy nuclei can be well reproduced.

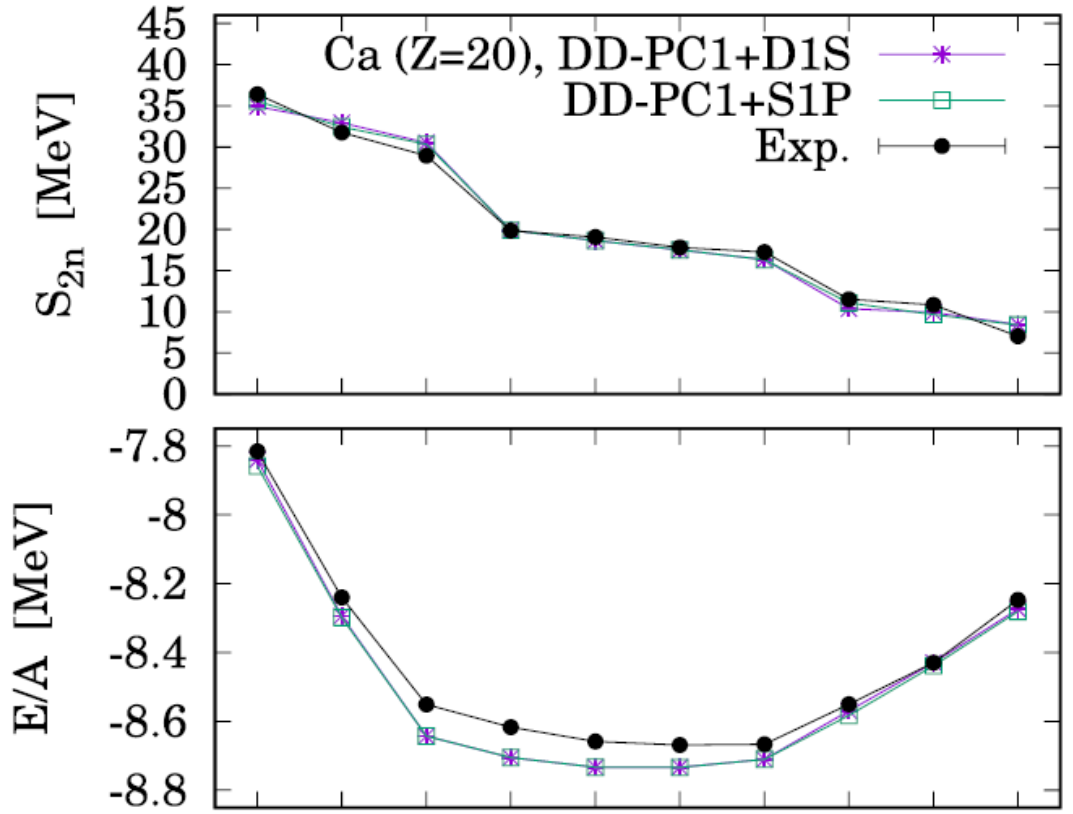

IV-PV interaction's effect on M1 (^{48}Ca)

$$\frac{dB_{M1}}{dE_\gamma} = \sum_f \delta(E_\gamma - \hbar\omega_f) \sum_\nu \left| \left\langle \omega_f | \hat{\mathcal{Q}}_\nu(M1) | \Phi \right\rangle \right|^2, \quad \text{with}$$

$$\mathcal{L}_{IV-PV} = -\hbar c \frac{\alpha_{IV-PV}}{2} \left[\bar{\psi}\gamma_5\gamma_\mu\vec{\tau}\psi\right] \left[\bar{\psi}\gamma_5\gamma^\mu\vec{\tau}\psi\right]$$

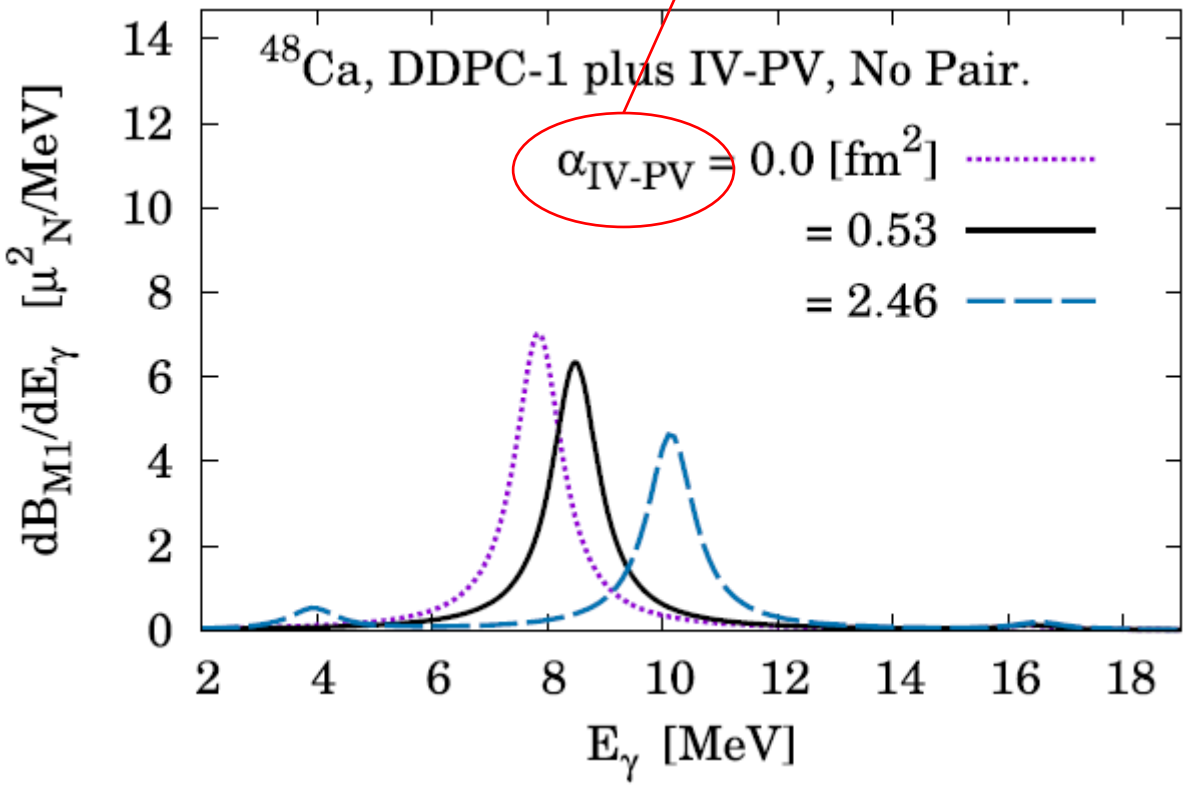

(1) DD-PC1 for ph-RHB;
(2) IV-PV (residual int.) for ph-RQRPA.
(3) Pairing vanishes.
➔ The IV-PV residual interaction noticeably affects the M1-transition energy.

Note: in the GS (0+) solutions from the RHB, the IV-PV does not make a finite effect.

Systematic calculations for M1 in Ca isotopes

T.O., G. Kruzic, N. Paar, J. Phys. G 47, 115106 (2020).

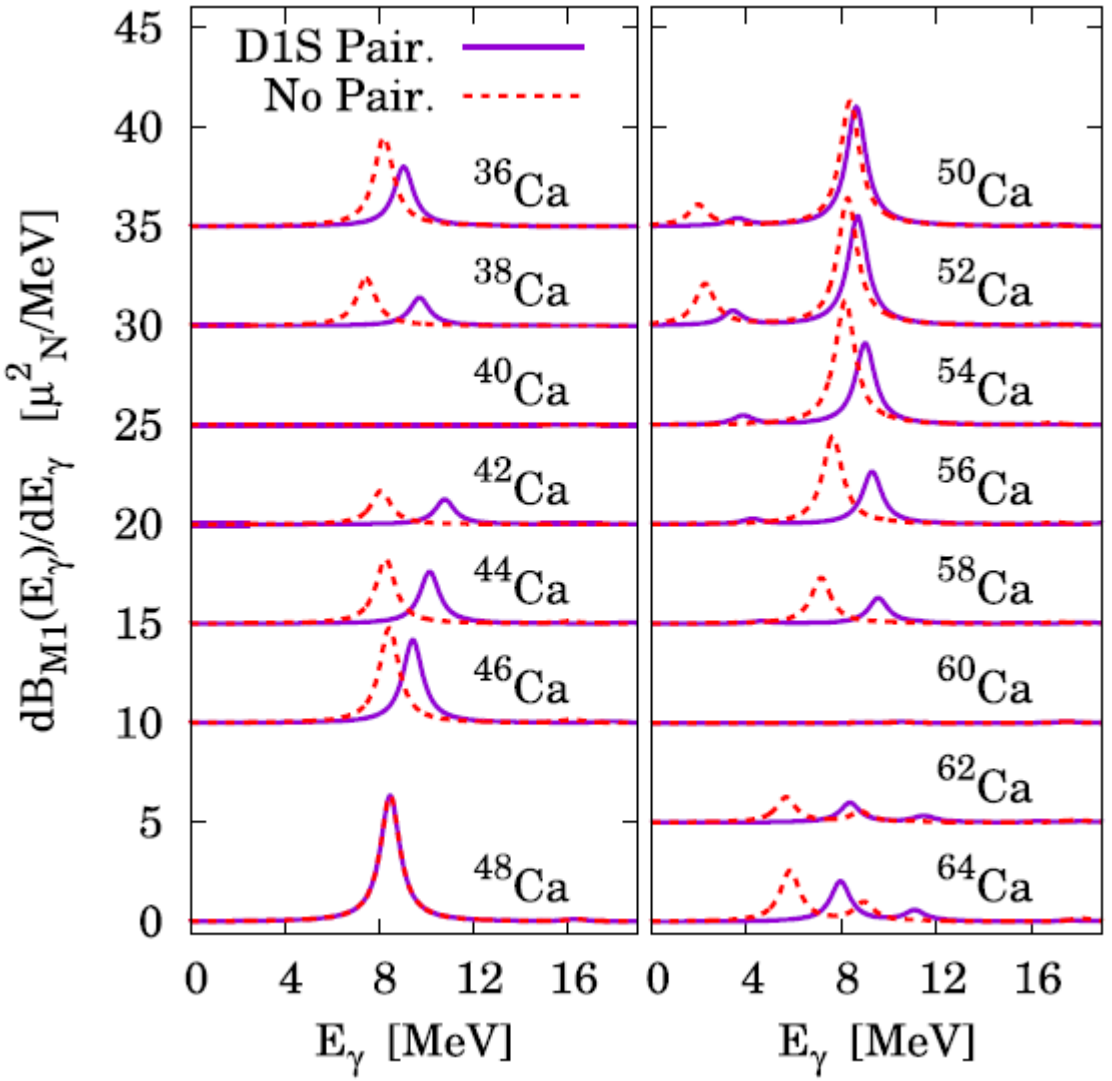

$$\frac{dB_{M1}}{dE_\gamma} = \sum_f \delta(E_\gamma - \hbar\omega_f) \sum_\nu \left| \left\langle \omega_f | \hat{\mathcal{Q}}_\nu(M1) | \Phi \right\rangle \right|^2,$$

For Ca nuclei, their M1 strengths have one or two-peak distributions. Each peak can be attributed to the
(f7/2)➔(f5/2),
(p3/2)➔(p1/2), or
(d5/2)➔(d3/2) transition.

Note: the LS-split gap does NOT coincides with the actual M1-excitation energy, because of the residual interactions.

LS-splitting gaps v.s. actual M1-excitation energies

T.O., G. Kruzic, N. Paar, J. Phys. G 47, 115106 (2020).

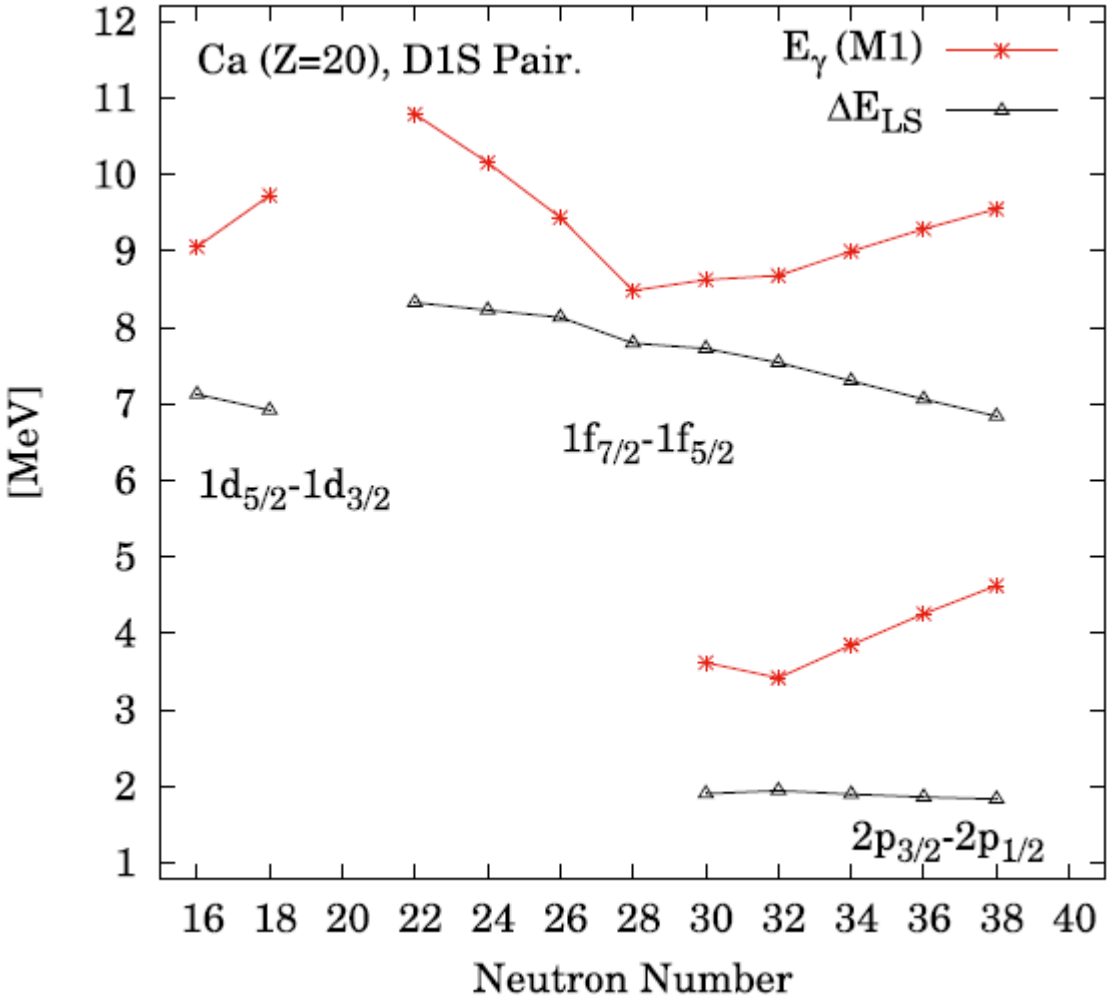

ΔE_{LS} ⇔ RHB ground states.

Eγ(M1) ⇔ QRPA.

$$\begin{pmatrix} A & B \\ B^* & A^* \end{pmatrix} \begin{pmatrix} X^{(\omega)} \\ Y^{(\omega)} \end{pmatrix} = \hbar\omega \begin{pmatrix} I & 0 \\ 0 & -I \end{pmatrix} \begin{pmatrix} X^{(\omega)} \\ Y^{(\omega)} \end{pmatrix}$$

What does make the difference?

➔ Residual interactions:

(1) IV-PV in ph channel;

(2) D1S-pairing in pp channel.

M1 in Sn isotopes

G. Kruzic, T.O., and N. Paar, PRC 103, 054306 (2021).

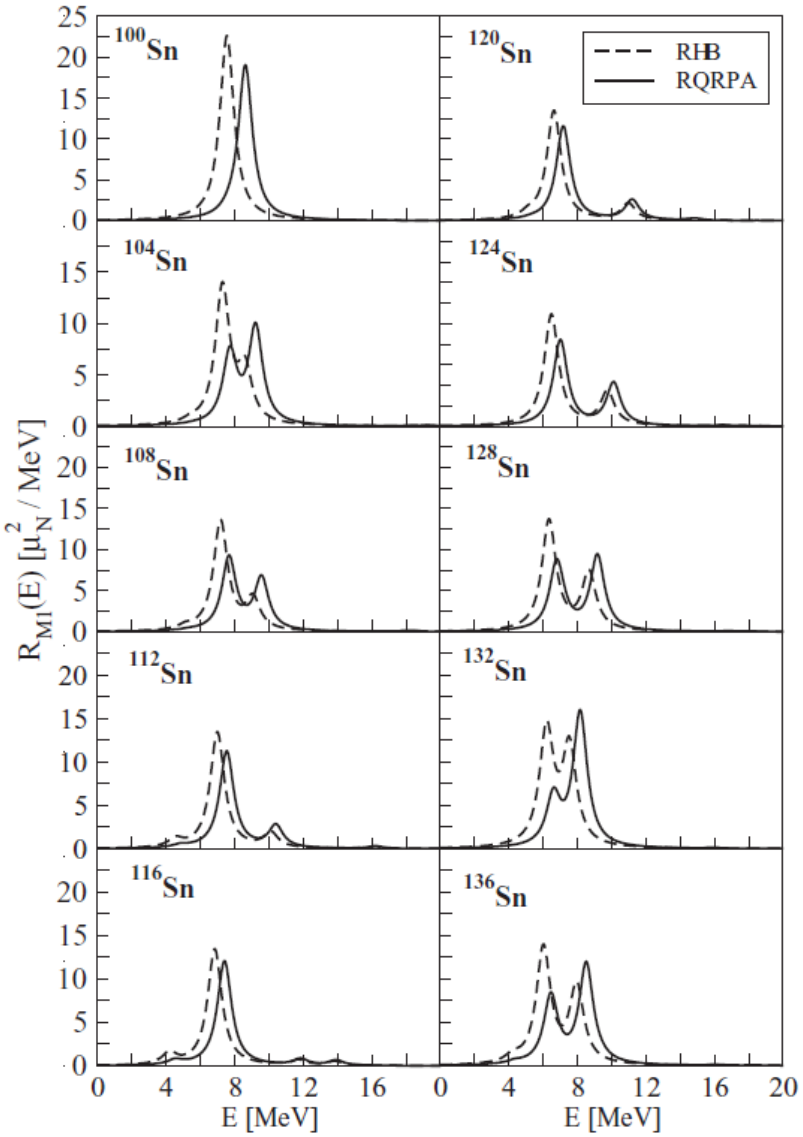

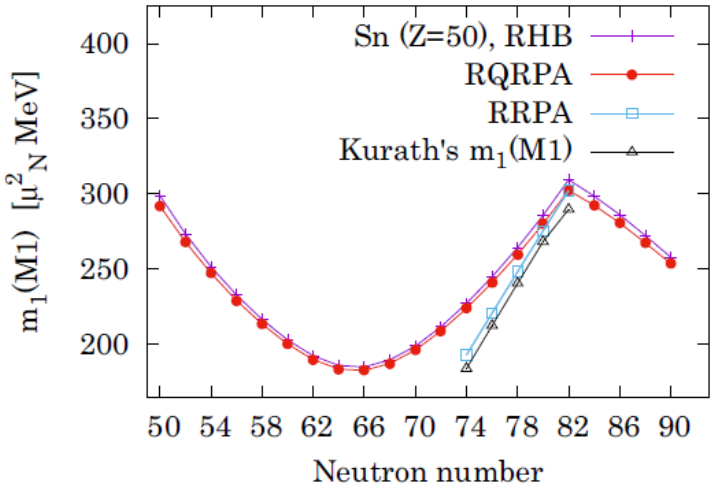

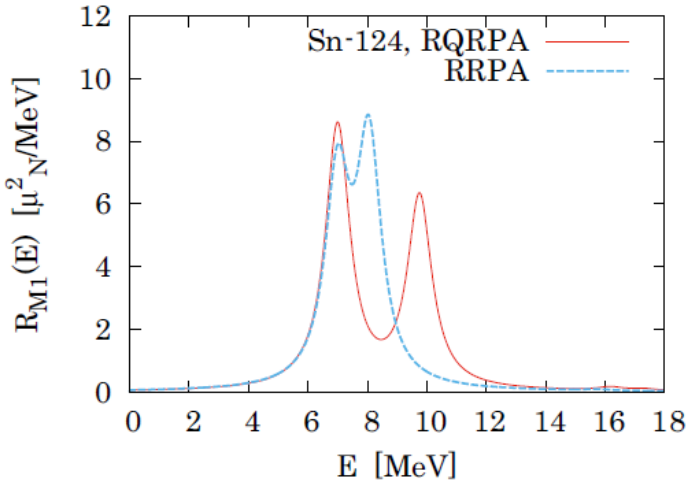

FIG. 7. (Top) Energy-weighted summation m_1(M1). For $^{124-132}$Sn, the corresponding results with Kurath's sum rule are also displayed. (Bottom) M1 strength distribution of ^{124}Sn with and without the pairing interaction.

Energy-weighted summation:

$$m_k(\mathrm{M1}) \equiv \int E_\gamma^k \frac{\mathrm{d}B_{\mathrm{M1}}}{\mathrm{d}E_\gamma}\,\mathrm{d}E_\gamma.$$

v.s. Kurath's sum rule in "D. Kurath, Phys. Rev. 130, 1525 (1963)":

$$m_1(\mathrm{M1},\ \mathrm{Kurath}) \cong \frac{3\mu_N^2}{4\pi}\left(g_s^{\mathrm{IV}} + g_l^{\mathrm{IV}}\right)^2 \sum_i (-a_{\mathrm{SO}})\langle \mathbf{l}(i)\cdot\mathbf{s}(i)\rangle,$$

➔ Around Sn-132, Kurath's M1 rule is good. Otherwise, because of the mixing of l & j components of valence neutrons, this rule does not simply apply.

➔ Neglecting the paring shifts the neutron's M1-excitation energy.

Proton inelastic scattering to probe M1

P. von Neumann-Cosel and A. Tamii, Eur. Phys. J. A 55, 110 (2019):

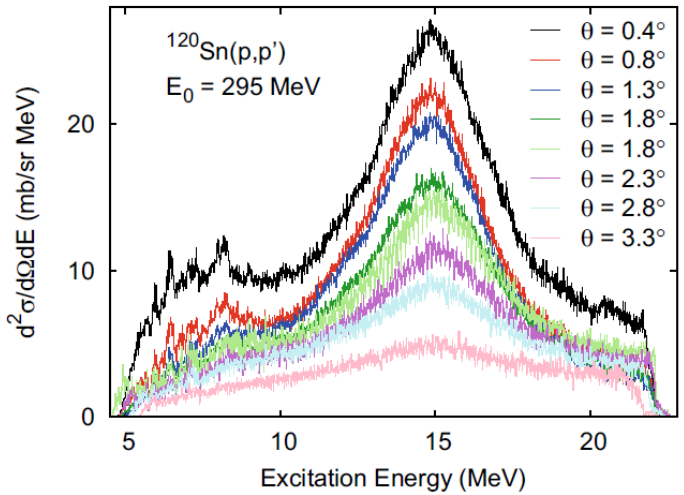

Fig. 11. Experimental cross sections of the ^{120}Sn(p, p′) reaction at $E_0 = 295$ MeV for different angle cuts. The top four spectra originate from a measurement with the central Grand Raiden spectrometer angle set to 0°, whereas the lower four were taken at 2.5°. Figure taken from ref. [147].

S. Bassauer et. al., Phys. Rev. C 102, 034327 (2020):
M1 data for Sn isotopes are obtained.

TABLE V. Neutron threshold energies S_n, $B(M1)$ strengths up to S_n, and total $B(M1)$ strengths up to energy E_{max} in ^{112,114,116,118,120,124}Sn deduced from the present data as described in the text.

	S_n (MeV)	$\sum_6^{S_n} B(M1)$ (μ_N^2)	E_{max} (MeV)	$\sum_6^{E_{max}} B(M1)$ (μ_N^2)
^{112}Sn	10.79	13.1(1.2)	11.2	14.7(1.4)
^{114}Sn	10.30	9.2(1.0)	12.8	19.6(1.9)
^{116}Sn	9.56	8.1(0.7)	11.8	15.6(1.3)
^{118}Sn	9.32	8.2(1.1)	11.2	18.4(2.4)
^{120}Sn	9.10	4.8(0.5)	12.4	15.4(1.4)
^{124}Sn	8.49	5.6(0.6)	11.4	19.1(1.7)

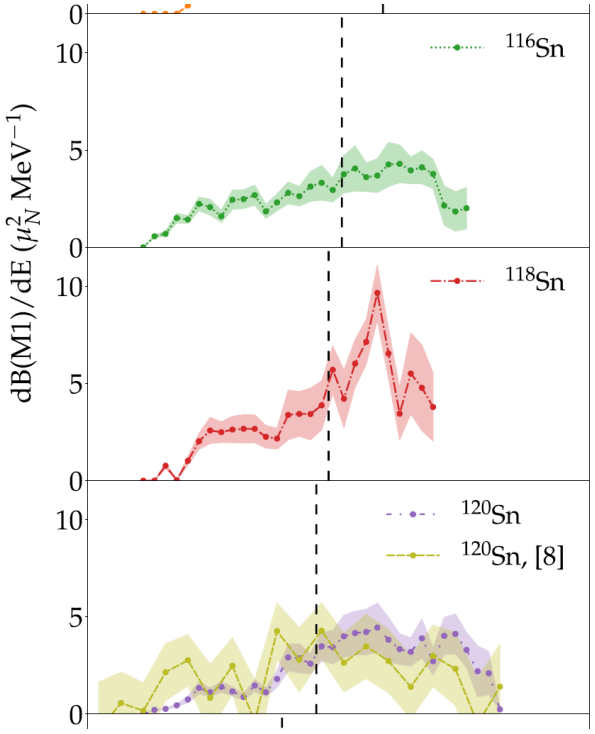

➔ These new data can be a good reference to examine & improve the REDF framework.

M1 summations of Sn isotopes and quenching effect

Our REDF-QRPA result

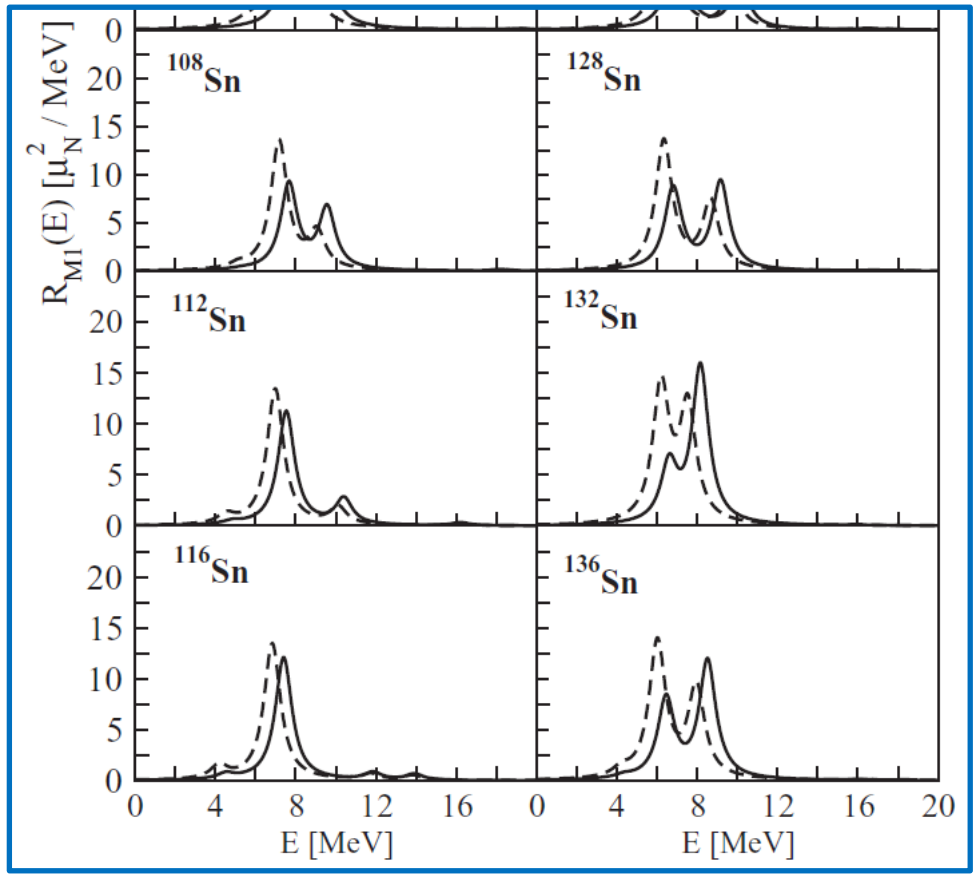

G. Kruzic, T.O., N. Paar, PRC 103, 054306.

➔ Summation of M1 strength:

	$\sum B_{M1}^{th.}$	$\sum B_{M1}^{exp.}$	g_{eff}/g_{free}
^{112}Sn	22.81	14.7(1.4)	0.80
^{114}Sn	22.61	19.6(1.9)	0.93
^{116}Sn	22.56	15.6(1.3)	0.83
^{118}Sn	22.76	18.4(2.4)	0.89
^{120}Sn	23.34	15.4(1.4)	0.81
^{124}Sn	25.55	19.1(1.7)	0.86

Exp. Data from S. Basseur et. al., PRC 102, 034327 (2020).

- ✓ Quenching of 0.8-0.9 is necessary to reproduce the exp. M1 summation, i.e., it is not bad.
- ✓ Experimental M1 distribution is quite broad, whereas our result is based on a narrow-resonance assumption.

➔ Further investigations are in process now.

App 2:
Sensitivity of M1 to pairing modes

Publication:
T.O., G. Kruzic, and N. Paar, The Eur. Phys. Journal A, 57, page 1-7 (2021).

Is S_{12}=0 or S_{12}=1 pairing mode dominant in nuclei?

S_{12}=0

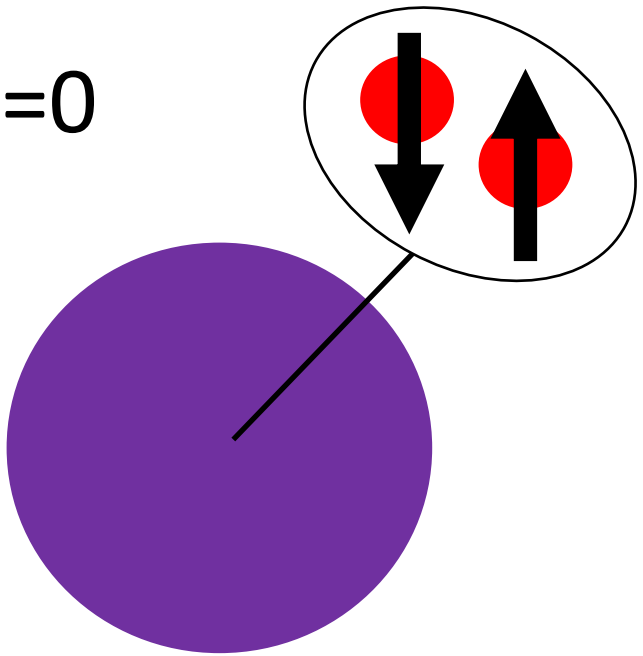

OR/AND

S_{12}=1

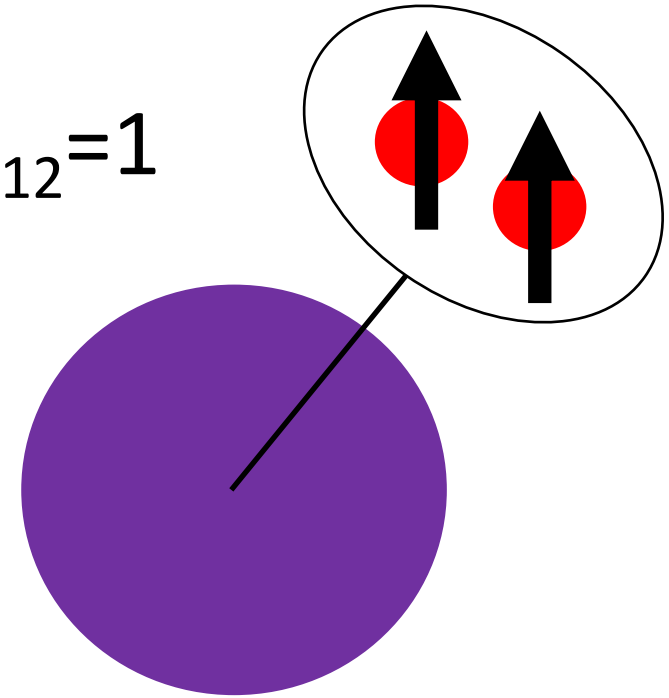

???

Like BCS coupling for electrons

Like Helium-3 superfluidity

➔ Studying the M1 response may resolve this pairing-mode problem.

Pairing-model dependence

(1) The same REDF-RHB & QRPA calculations are employed: ph-Lagrangian = DD-PC1 + IV-PV.

(2) We investigate the M1 response of open-shell nuclei with the Gogny pairing interaction in the pp channel of the relativistic QRPA. Two types of the Gogny central force, D1S and S1P, are compared.

Gogny potential:

$$V_{\rm pp} = \sum_{i=a,b} \left\{ (W_i - H_i) + (B_i - M_i)\hat{P}_\sigma \right\} e^{-\frac{d^2}{\mu_i^2}},$$

D1S ➔ S_{12}=0 pairing is dominant.

S1P ➔ S_{12}=1 pairing is dominant.

➔ For the RHB-GS solutions, D1S & S1P show no difference.

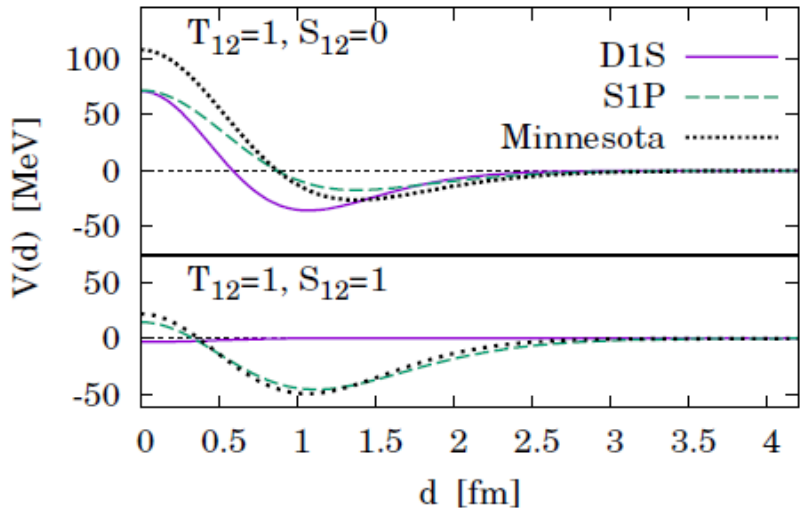

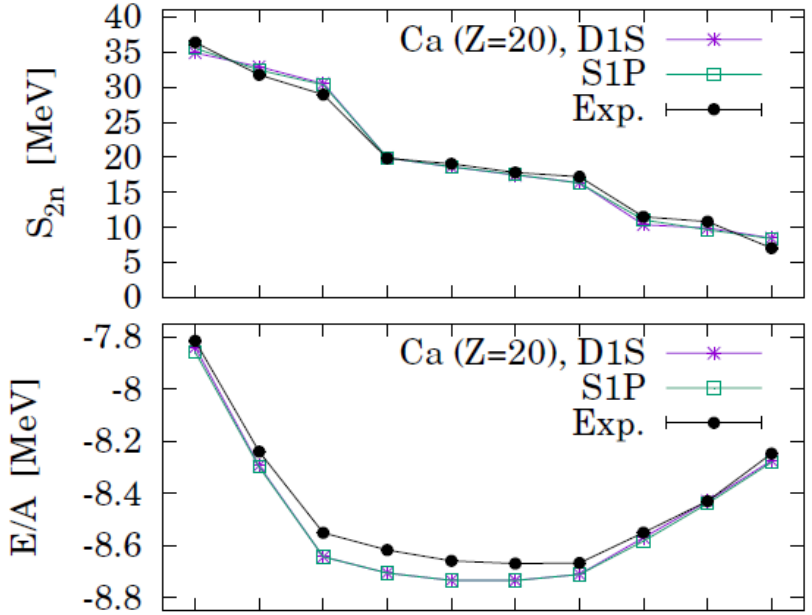

T.O., G. Kruzic, and N. Paar, EPJA 57, 1-7 (2021).

Pairing-model dependence

D1S ➔ S_{12}=0 pairing is dominant.
S1P ➔ S_{12}=1 pairing is dominant.

However, for the M1-excited states, the D1S and S1P predict the different results.

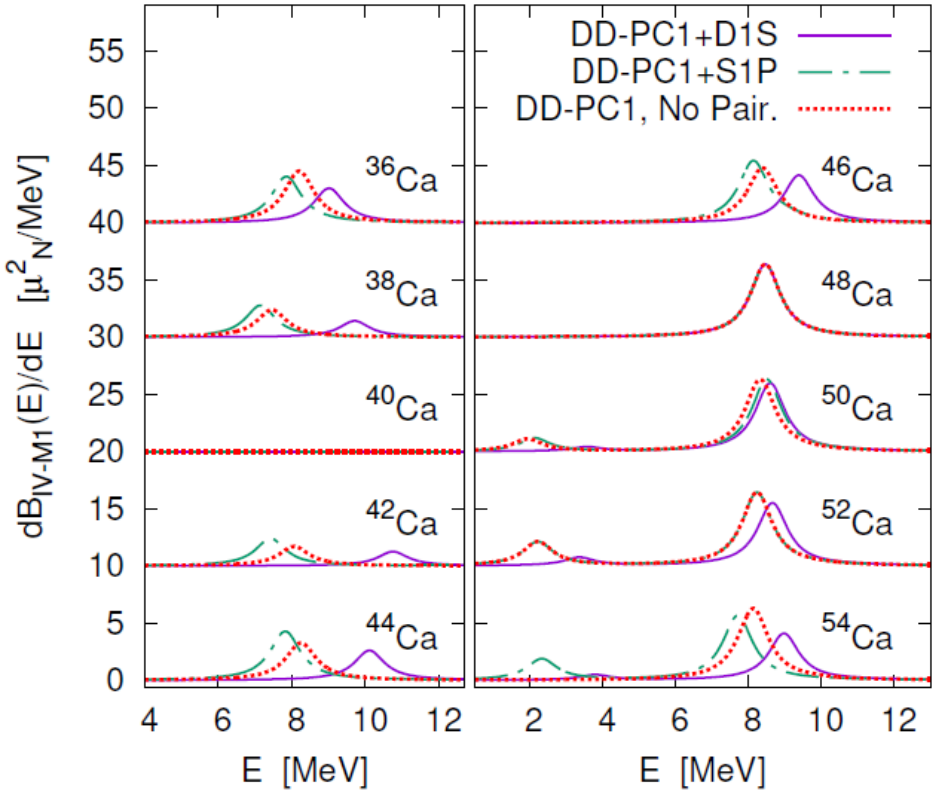

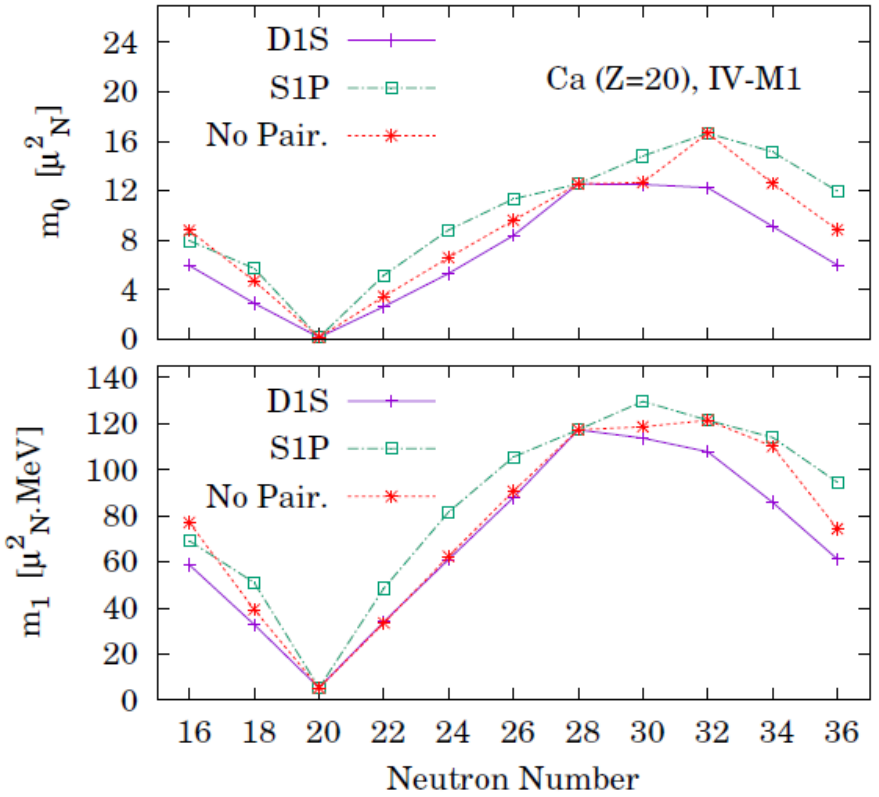

FIG. 3. The IV-M1 strength ($0^+_{GS} \longrightarrow 1^+$) in the DD-PC1 plus D1S pairing, plus S1P pairing, and no pairing cases for Ca isotopes.

M1 ⇔ Coupled spin (S_{12}) of nuclear pairing

Link of M1 summation with pairing

T.O., G. Kruzic, N. Paar, J. Phys. G 47, 115106 (2020).

(We only consider the neutron's M1 excitation here.) The 0th summation of M1 is given as

$$m_0 \equiv \sum_{\nu}\sum_{E}\left|\left\langle E\right|\left(g_l\hat{L}_\nu + g_s\hat{S}_\nu\right)\left|i\right\rangle\right|^2$$

$$= \left\langle i\right|\left(g_l\hat{\mathbf{L}} + g_s\hat{\mathbf{S}}\right)^2\left|i\right\rangle . \qquad \hat{L}_\nu = \sum_{k\in N}\hat{l}_\nu^{(k)} \text{ and } \hat{S}_\nu = \sum_{k\in N}\hat{s}_\nu^{(k)}$$

Then, by using the notation J=L+S (total angular momentum),

$$m_0 = g_l(g_l - g_s)\left\langle\hat{\mathbf{L}}^2\right\rangle_{[i]} + g_s(g_s - g_l)\left\langle\hat{\mathbf{S}}^2\right\rangle_{[i]} + g_lg_s\left\langle\hat{\mathbf{J}}^2\right\rangle_{[i]}.$$

For the GS of even-even nuclei with $J_i^P=0^+$, the allowed components are of (L=S), only. Therefore,

$$m_0 = \sum_{(L,S)}\delta_{L,S}|C_{(L,S)}|^2\left\{g_l(g_l - g_s)\cdot L(L+1) + g_s(g_s - g_l)\cdot S(S+1)\right\}$$

$$= \sum_{S}|C_{(L=S,S)}|^2(g_l - g_s)^2S(S+1).$$

If the (s_{12}=0) mode of pairing is dominant, the total spin S is 0, too. ➔ m_0 is small. Otherwise, including the non-zero S components, the m_0 value can be enhanced.

REDF-QRPA v.s. experimental M1 data

M1 response of open-shell nuclei with (i) DD-PC1 REDF (Gogny pair.) for the ph (pp) channel, and (ii) DD-PC1 plus IV-PV REDF (Gogny pair.) for the ph (pp) channel of the relativistic QRPA.

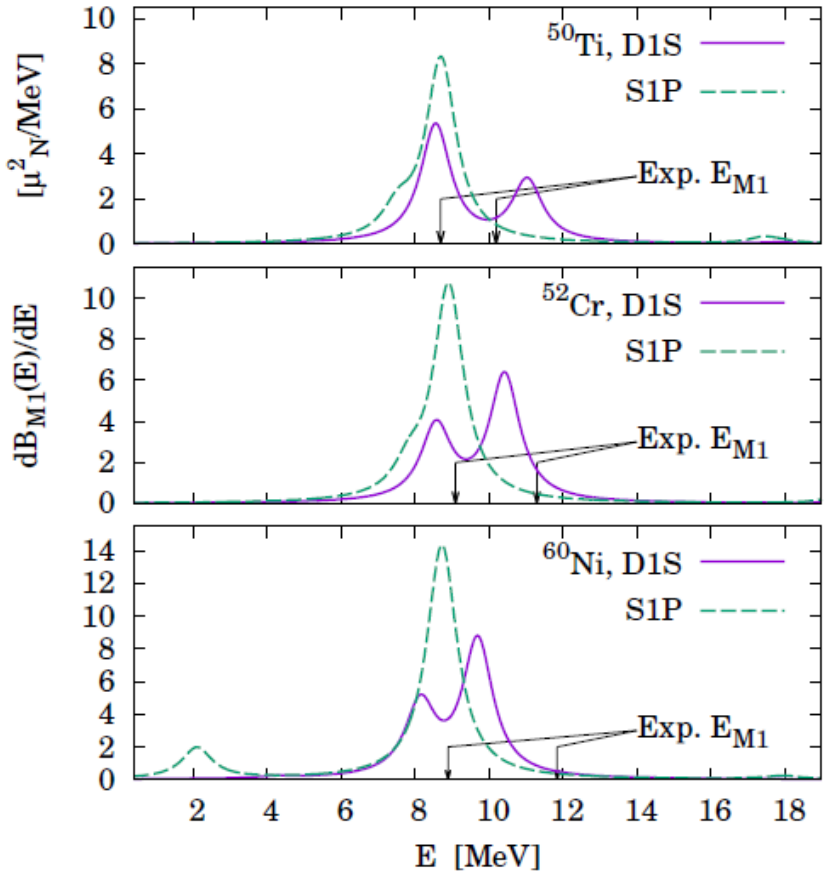

Exp. Data = D. I. Sober, et al, Phys. Rev. C 31, 2054 (1985).

Gogny-pairing interactions:

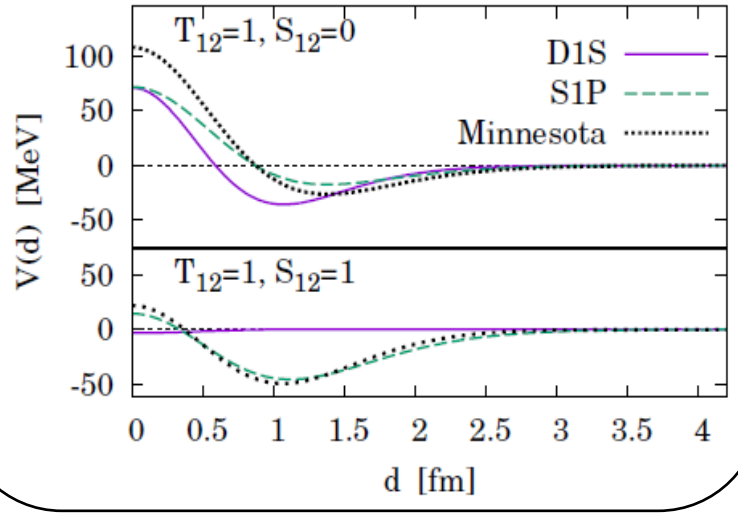

- ✓ S_{12}=0 looks as the better option to qualitatively reproduce experimental M1 data. S_{12}=1 pairing picture has not been validated in our result.
- ✓ Systematic M1 data can provide an evidence of the Cooper-pairing mode(s) inside nuclei.

How about it in other modes?

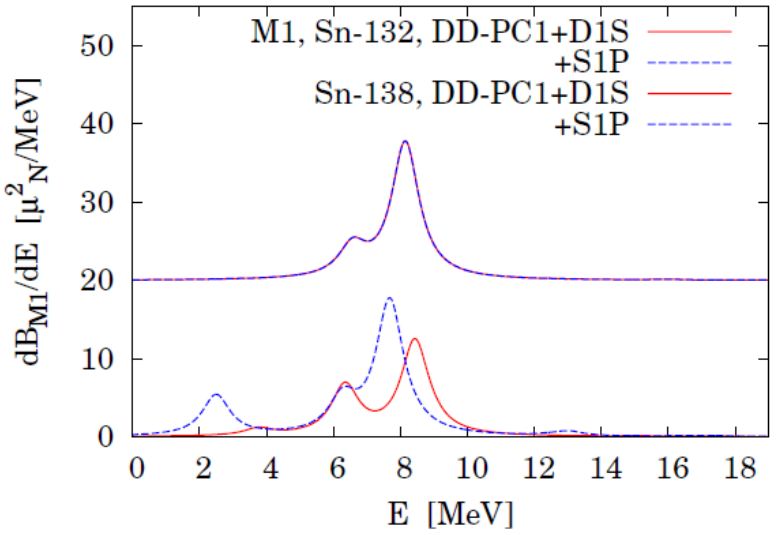

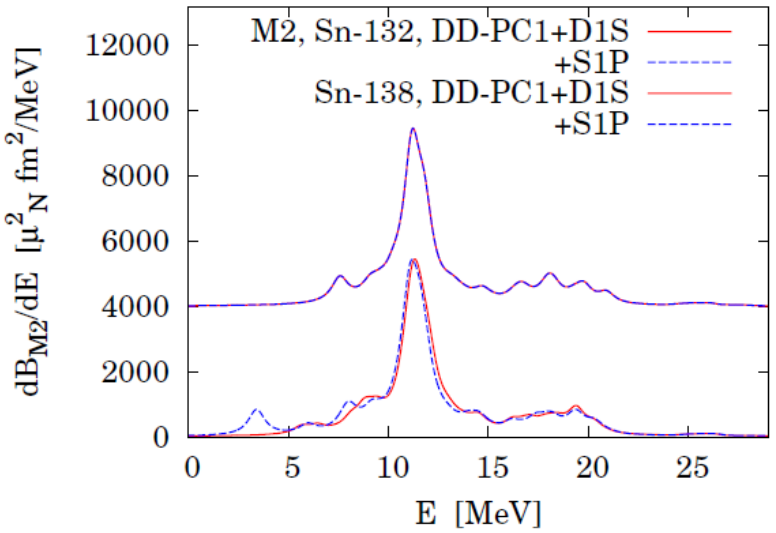

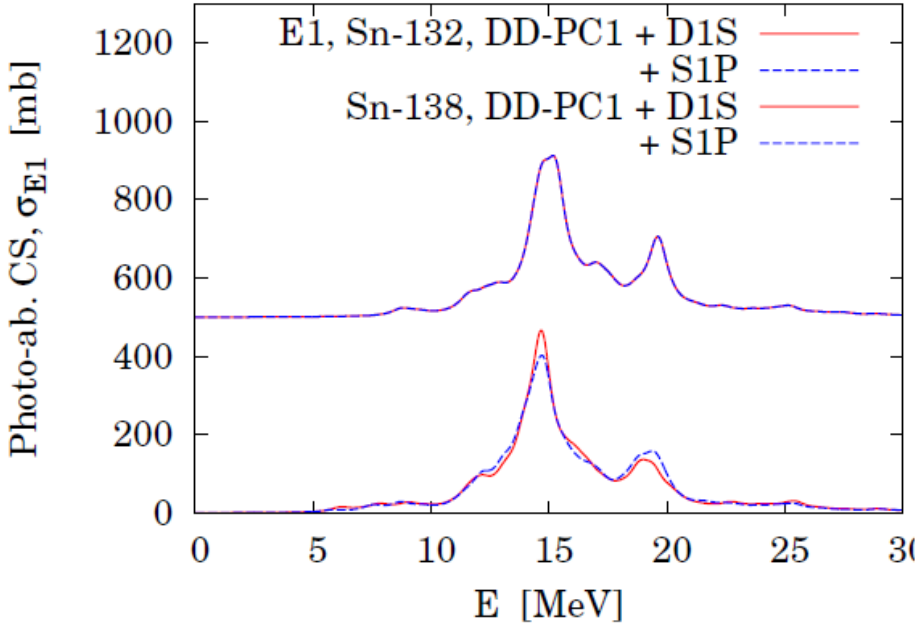

Test of RQRPA in E1:

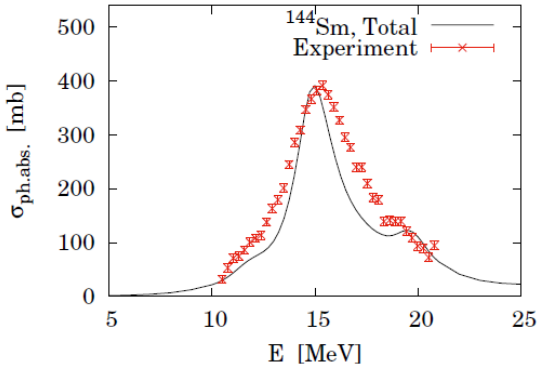

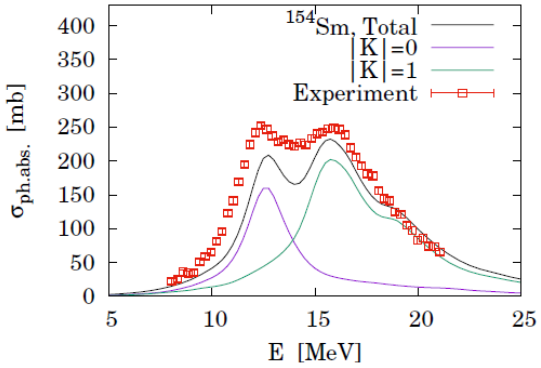

➔ M1 is especially sensitive to pairing modes.

➔ M2 with S1P yields the low-lying resonance.

➔ E1 is not sensitive. This insensitivity is checked also in E2 and E3.

Basic knowledge on EDF theory

Hohenberg-Kohnの定理（電子系）　　Phys. Rev. 136, 8844 (1964).
多体系の基底状態Φとそのエネルギーは、密度$\rho(x) = \langle\Phi|\psi^+(x)\psi(x)|\Phi\rangle$の汎函数であり、エネルギー汎函数$\mathrm{E}[\rho(x)] = \langle\Phi[\rho]|\hat{H}|\Phi[\rho]\rangle$が分かれば、密度に関する変分原理から、基底状態が求まる。

Kohn-Sham理論（電子系）　　Phys. Rev. 140, A1133 (1965).
電子多体系について、Kohn-Sham方程式という形で「密度に関する変分原理」計算が実行可能であることを示した。

原子核のEDF
- (1970~)現象論としての平均場計算。有効核力としてSkyrme, Gogny, Rela’ point-coupling, etc.が用いられる。
- (2000~)上記の計算法が密度汎函数理論の実装例として解釈されるようになる。